LA-UR- 09-03033

Approved for public release; distribution is unlimited.

Title: Delayed-Gamma Signature Calculation for Neutron-Induced Fission and Activation Using MCNPX. Part I: Theory.

Author(s): Joe W. Durkee, Jr., Michael R. James, Gregg W. McKinney, Holly R. Trellue, Laurie S. Waters, and William B. Wilson

Intended for: Progress in Nuclear Energy

Los Alamos
NATIONAL LABORATORY
EST. 1943

Los Alamos National Laboratory, an affirmative action/equal opportunity employer, is operated by the Los Alamos National Security, LLC for the National Nuclear Security Administration of the U.S. Department of Energy under contract DE-AC52-06NA25396. By acceptance of this article, the publisher recognizes that the U.S. Government retains a nonexclusive, royalty-free license to publish or reproduce the published form of this contribution, or to allow others to do so, for U.S. Government purposes. Los Alamos National Laboratory requests that the publisher identify this article as work performed under the auspices of the U.S. Department of Energy. Los Alamos National Laboratory strongly supports academic freedom and a researcher's right to publish; as an institution, however, the Laboratory does not endorse the viewpoint of a publication or guarantee its technical correctness.

Form 836 (7/06)

DELAYED-GAMMA SIGNATURE CALCULATION FOR NEUTRON-INDUCED FISSION AND ACTIVATION USING MCNPX. PART I: THEORY.

by

Joe W. Durkee, Jr.; Michael R. James; Gregg W. McKinney; Holly R. Trellue; Laurie S. Waters; and William B. Wilson
Los Alamos National Laboratory
jdurkee@lanl.gov
505-665-0530
Fax: 505-665-2897
PO Box 1663, MS K575
Los Alamos, NM 87545

ABSTRACT

The capability to conduct automated radiation transport simulations of delayed-gamma emission spectra at discrete (line) energies created by the products of neutron fission and activation has been developed for MCNPX. To do so, the CINDER'90 isotopic transmutation code has been merged into MCNPX to seamlessly supply time-dependent, decay-chain atom densities for 3400 nuclides. A new dataset containing ENDF/B-VI emission probability line data for 979 nuclides has been created for MCNPX, with the balance of the 3400 nuclides treated using existing 25-group emission spectra. Cumulative distribution sampling functions have been developed to accommodate line and multigroup emission data. Fission-product sampling for fissions induced by sub-20-MeV neutrons uses fission-yield data for thermal ($E < 1$ eV), fission-spectrum (1 eV $\leq E < 14$ MeV), and high-energy ($E \geq 14$ MeV) neutrons for isotopes of

uranium, plutonium, thorium, americium, californium, curium, einsteinium, fermium, and neptunium. For higher-energy neutrons, LAHET, a physics package that is also a part of MCNPX, generates a list of residual nuclides. In Part II, we present simulation results for models based on experiments conducted by Fisher and Engle (1964) and Beddingfield and Cecil (1998) to validate the new capability. As will be seen therein, the MCNPX results are in good agreement with the measured data. Finally, in Part III we augment the Monte Carlo presentation with a transport-theory formulation to provide a succinct encapsulation of the relevant physics. The new MCNPX delayed-gamma development offers a powerful new tool for fission-related signature recognition.

KEYWORDS: MCNPX; CINDER'90; fission-product; delayed-gamma; activation; lines.

1. INTRODUCTION.

The emission of gamma radiation due to the decay of radioactive fission products has been of interest since the dawn of the nuclear age (Roberts et al., 1939). O. R. Frisch and co-workers conducted the earliest work involving enriched material using a pulsed fission source (the "drop" or "dragon" system) at Los Alamos National Laboratory (LANL) in early 1945 to study delayed-neutron and gamma behavior (Frisch, 1945; de Hoffmann et al., 1948; Moon, 1945;[†] Malenfant, 2005).

[†] This reference includes one figure that presents integral delayed-gamma detector response from 18 to 1000 s for the Chicago pile. However, no emission spectra were reported.

Since that time, theoretical work has been done to characterize delayed-gamma behavior (Way and Wigner, 1948; Griffin, 1964; Katakura and England, 1991). Additional experimentation has been conducted to acquire and tabulate data, with the first detailed experimental study conducted by Maienschein et al. (1958) at Oak Ridge National Laboratory. Later, experimental work was conducted at LANL (Engle and Fisher, 1962; Fisher and Engle, 1964; Keepin, 1965) and elsewhere (Battat et al., 1968; Moore, 1969; Erdtmann and Soyka, 1979; Jurney et al., 1979).

More recently, advances in gamma-ray spectroscopy have yielded measured spectra with energy resolution that is sufficient to permit fission material and fission-product identification (at least for non-shielded applications). Experimental results obtained using high-purity germanium (HPGe) detectors for gamma-ray signature recognition have been reported for active-interrogation of ^{235}U and ^{239}Pu by thermal neutrons (Beddingfield and Cecil, 1998; Tipnis et al., 1998; Norman et al., 2004).

Applications involving delayed-gamma behavior include health physics (Morgan and Turner, 1973; Szasz, 1984; Goudsmit, 1988), material assay (Hollas et al., 1987; Pruet et al., 2004; Norman et al., 2004; Slaughter et al., 2005), sensor protection (Spletzer, 1992), and facility design (Henderson, et al., 1988; Liew and Ku, 1991; Guung et al., 2002) and calibration (Ma et al., 1996). High-altitude instrumentation design for environments involving hadronic interactions with radioisotope production and delayed-gamma emission are also of interest (Weidenspointer et al., 2005). The detection of nuclear

weapons and special nuclear material by means of active interrogation is evoking great interest (Siciliano et al., 2005).

Earlier Monte Carlo developmental work (Estes et al., 1988) done at LANL began to address the issue of automating the process of discrete-line gamma emission for arbitrary configurations of radioactive materials. That effort was not intended to accommodate fission products per se. Moreover, it did not explicitly treat the temporal variation of isotopic inventories, so the feature lacked a truly time-dependent capability.

Recent work has been reported (Pruet et al., 2004) regarding detailed delayed-gamma-emission Monte Carlo simulations. That work is reported to treat neutron-induced fission using 1000 decay nuclides and 20000 discrete emission energies, but the authors concluded that the complete Monte Carlo simulation of fissioning systems, including nuclide production and decay and transport of their decay radiations, is not currently directly possible.

The MGGPOD code (Weidenspoitner et al., 2005) is a newly developed GEANT-based simulation package that includes the ORIHET code as a means of calculating isotopic chains. However, this package appears to be designed for applications other than fissioning systems.

The SCALE 5.0 package (Klingensmith and Gauld, 2005) has been released with upgrades to its master photon library that include the treatment of 2101 nuclides and

115000 discrete lines for short- and long-live isotopes. Calculated and measured photon-emission spectra resulting from ^{235}U irradiation in a thermal-neutron flux exhibit very good agreement for post-fission times ranging from 2.7 to 9950 s.

Here we give a detailed accounting of upgrades to LANL's MCNPX Monte Carlo radiation-transport code that enable the automated calculation of time-dependent emission and transport of gamma rays created as a result of neutron-induced fission and activation. Whereas earlier work treated gamma emission using multigroup data (Trellue et al., 2005), the new upgrade accommodates emission via discrete lines. The upgrade involves the linkage of MCNPX, CINDER'90 (Wilson et al., 1995), and the necessary data files to streamline the calculation of time-dependent, fission-product nuclide densities. The CINDER'90 data library has been upgraded to include ENDF/B-VI gamma-line emission spectra for 979 radionuclides. The upgrade includes an interface with the Los Alamos High-Energy Transport (LAHET) package to enable the treatment of high-energy (>20-MeV) neutrons. A derivation of the delayed-gamma sampling equations is presented, and a discussion of the MCNPX treatment of coupled neutron-photon transport, inclusive of prompt and delayed contributions, is included. The delayed-gamma upgrades reported here began to appear in MCNPX version 2.5.0, and continue with subsequent version as well as beta releases.

2. MCNPX, CINDER'90, AND LAHET CODE OVERVIEWS.

MCNPX is a LANL Monte Carlo (Pelowitz, 2008) radiation-transport code that has capabilities that include three-dimensional (3D) geometry modeling, continuous-energy transport, transport of 34 different particle types, a variety of source and tally options, interactive graphics, and support for a variety of sequential and multiprocessing computer platforms. MCNPX has several powerful variance-reduction techniques that enhance computational performance. MCNPX is written in Fortran 90, has been parallelized, and works on platforms including single-processor personal computers (PCs), Sun workstations, Linux clusters, and supercomputers.

MCNPX emits and transports "particles" (radiation quanta) given a user-supplied model (input deck) that contains specifications of the geometry,* material, source, cross-section, and particle type(s) to be transported. These data are used along with code-supplied data to calculate integral quantities, referred to as cumulative distribution functions ("CDFs"), in energy, time, and direction. These distributions are sampled to emit particles.

Use of the prior versions of MCNPX for fission-product, delayed-gamma-line-emission calculations would be overwhelmingly complicated. The difficulty arises from the need to specify time-dependent isotopic concentrations for each fission product and its associated radioactive decay progeny and to treat the associated large numbers of emission lines. Consequently, the new upgrade has been designed to automate the

* MCNPX uses "cells" as the geometry building blocks. Each cell contains a spatially uniform material that consists of one or more nuclides. The notation used throughout this paper omits explicit cell-wise spatial variation with the note that MCNPX accommodates source heterogeneity on a cellwise basis.

treatment of the isotopic concentrations and the emission lines given only user-specified material compositions, the irradiating source specifications, and the use of a single flag in the input deck (to signal feature use). The new capability then automatically calculates and uses isotopic concentrations, decay constants, and line emission probabilities for each radionuclide that is created by a fission event to compute CDFs that are sampled for the delayed-gamma quantity, energy, and emission time following a fission event.

Neutron-induced fission creates a mass distribution of fission products that is aptly characterized by the familiar "double-hump" profile (Keepin, 1965, pp. 21–27; Lamarsh, 1972; Henry, 1975). This profile varies in its shape, depending on the fissioning nucleus, incident particle type, and the energy of the incident particle. Many of these fission products are unstable and decay by beta emission—frequently with the emission of neutrons and photons.

In MCNPX, fission-product determination is based on the fissioning species, as well as on the type and energy of the source particle that induces fission. For neutrons with energies up to 20 MeV, the classical fission-product yield curve data are randomly sampled. Fission-yield sets are available (England and Rider, 1994) for a variety of nuclides and evaluations made using thermal ($E \leq 1$ eV), fission-spectrum (fast; 1 eV < E < 14 MeV), and high-energy (≥ 14 MeV) neutron spectra. Functionally, this determination process occurs in the new "interface" routine **CINDER_INTERFACE_DELAYEDNG** ("**CID**"), which links MCNPX to CINDER'90 (see Fig. 1a in the Appendix). The data file cinder.dat contains 1325 fission-

yield sets. The identity of the first fission product is determined in **CID** by sampling the appropriate yield curve. The prospective second fission product is determined by mass conservation. The prospective second fission product is used if data exists in cinder.dat; otherwise, a "nearest-neighbor" search is made in atomic mass ("A") until a second fission product for which cinder.dat data exists is found.

For neutrons with energies above 20 MeV, or for photons with energies sufficient to induce photofission, the LAHET package, which was integrated into MCNPX in an earlier effort (Wilson et al., 1993; Waters, 1999), determines the reaction byproducts, or "residual nuclides." This list is forwarded to **CID**, with the nuclides used in the call to CINDER'90 for the calculation of their associated decay-product data.

Once each fission product or residual nuclide is determined, its identity is sent from **CID** to CINDER'90 (Wilson et al., 1995). CINDER'90 then generates the decay data for all of the radionuclides in the decay chain for a fission product. CINDER'90 is a nuclear transmutation code that calculates isotopic inventories in spatially homogeneous regions created by neutron transmutation and radioactive decay. Because the type and number of source and loss paths can vary from nuclide to nuclide, the corresponding differential equations can differ in structure, making a general solution difficult to obtain. CINDER'90 solves these equations using a decomposition scheme (England et al., 1976), wherein "partial" concentrations involve only a single-source term, but all loss mechanisms. The partial-concentration equations are described by a single set of coupled differential equations where the uniform structure allows for a single analytic solution

(assuming constant-flux conditions during a time increment). Once the partial concentrations are calculated, the total isotopic concentrations can be readily calculated.

Earlier CINDER versions required the *a priori* stipulation of all nuclides and transmutation pathways of interest. This information was incorporated into a set of chains tailored to specific applications (Wilson et al., 1995). CINDER'90 imposes no such constraint. Instead, CINDER'90 follows all paths associated with a nuclide until significance tests have failed. CINDER'90 accommodates 3400 nuclides with atomic numbers (Z) ranging from 1 to 103.

Originally written as a standalone code, CINDER'90 has been integrated into MCNPX to provide seamless simulation capability for delayed-gamma emission calculations. The delayed-gamma upgrades have been written so that a user can supply a conventional MCNPX input file for execution. There is no need to either include complicated source-card information (as was the case with Estes et al., 1988) or deal with standard interface files and execution scripts.

Section 5 contains a description of MCNPX delayed-gamma sampling theory. Before considering this theory, the delayed-gamma data are discussed in the following section.

3. MCNPX DELAYED-GAMMA DATA.

The MCNPX delayed-gamma emission-spectra data consist of two structures: multigroup and line. All data are ENDF/B-VI based.

The multigroup library is the most comprehensive dataset. These emission data are available in a 25-group format for 3400 radionuclides, and the data reside in file cinder.dat (distributed with MCNPX).

Line data have been obtained from the LANL Nuclear Information Service (located at http://t2.lanl.gov/data/data.html); these data have been extracted from the ENDF/B-VI evaluation. Radioactive-decay data for 979 radionuclides have been aggregated into the file cindergl.dat. These data include lower-energy photons, referred to as x-rays in these files. Throughout this paper, the term "photon" is used interchangeably to connote gamma and x-ray, and the use of "gamma" is meant to include x-ray.

The spectral-emission line data comprise discrete lines and "continuous" formats. For some radionuclides, all data are discrete; for others, it is continuous, and for the remainder, it is a combination of both discrete and continuous formats. Table 1 delineates the data composition.

The gamma-emission data reflect augmentation of measured ENDF/B-V data by calculated spectra (Katakura and England, 1991). The augmentation effort was conducted because it was recognized that reported measured emission data lacked a significant contribution of all gamma rays emitted by fission products. In particular, it was noted that the measured decay heat values exceeded calculated estimates. The disagreement was ameliorated by augmenting the measured data with calculated spectra based on

theoretical models for all of the ENDF/B-V nuclides decaying by beta emission. The continuous data appear in the data files in the form of differential emission values with a 10-keV bin structure.

Table 1. Line-data composition for 979-radionuclide delayed-gamma dataset

Composition by Data Component		
Data component		**Quantity**
Total		282,035
Discrete		24,199
Continuous		257,836
File size (lines)		747,730
Composition by Nuclide		
Data component	**Nuclides**	**Quantity**
Discrete only	526 (54%)	19,821
Continuous only	292 (30%)	214,293
Discrete and continuous mix	161 (16%)	47,921 total 4378D, 67742C[a]

[a]D and C connote discrete and continuous data types.

The MCNPX delayed-gamma upgrades have been developed based in part on the following considerations. First, the ability is retained to execute calculations using exclusively multigroup emission data. This ability permits comparison to line-data results, and is faster when lower-fidelity results are desired. Second, because the line data are available for a subset of the multigroup data, the upgrades for line-emission execution have had to accommodate a mixture of line and multigroup data. Line-emission execution is done by using line data for nuclides having such data and using multigroup data for the remainder of the radionuclides.

This complicated assortment of data has caused corresponding complexity in the development of sampling distributions and computer code. The sampling distribution development is discussed in Section 4.

4. THEORY OF MCNPX DELAYED-GAMMA EMISSION SAMPLING.

The creation of delayed gammas in MCNPX is done by randomly sampling probability distributions to determine their emission energy, time (delay time following fission), and direction. Currently, isotropic directional sampling is used. As such, the following development pertains to the energy- and time-dependent sampling schemes.

The development—including input processing, sampling-distribution theory, and coding—is complicated in MCNPX by virtue of the nature of the delayed-gamma emission data. In particular, CINDER'90 treats 3400 radionuclides for multigroup emission, whereas the LANL Nuclear Physics group (T-16) has line data available for

only 979 radionuclides. Consequently, the development and coding must accommodate probability distributions for this mixture of multigroup and line data.

This section presents the details of the theory and code development. A derivation of the multigroup sampling used in MCNPX has not be reported heretofore, so it is included below, along with development for line sampling.

As a preface, a brief review of relevant basic statistical principles regarding random number generation from probability distributions (Bevington and Robinson, 1992) is given.

4.1. Statistical distribution sampling theory.

Let $p(r)$ denote random numbers drawn from a probability density distribution that is uniform between $r = 0$ and $r = 1$ so that

$$p(r) = \begin{Bmatrix} 1 & \text{for } 0 \le r < 1 \\ 0 & \text{otherwise} \end{Bmatrix}. \tag{1}$$

This distribution is normalized so that

$$\int_{-\infty}^{\infty} p(r)dr = \int_0^1 1\,dr = 1. \tag{2}$$

Now suppose that random numbers are required from another distribution $P(x)$. The following steps show how to obtain a random number from $P(x)$ in terms of a random number drawn from $p(r)$. The principle of conservation of probability requires that

$$| p(r)dr | = | P(x)dx | . \tag{3}$$

Therefore,

$$\int_{-\infty}^{r} p(\tilde{r})d\tilde{r} = \int_{-\infty}^{x} P(\tilde{x})d\tilde{x} , \tag{4}$$

from which the following general result is obtained:

$$r = \int_{-\infty}^{x} P(\tilde{x})d\tilde{x} . \tag{5}$$

The integral is the CDF. Thus, given a random number r from a uniform distribution, the value of x that satisfies the integral in Eq. (5) is the value x that is randomly selected from the probability distribution $P(x)$.

Sampling the CDF, or generating the random variable x given r, is done using the inverse transform method. If $P(x)$ is analytical, in some instances the integral can be evaluated and the resulting expression inverted so that a solution for x in terms of a given r can be obtained in closed form. In other instances—such as delayed-gamma emission in

MCNPX—the distribution $P(x)$ is either piecewise continuous or discrete, depending on whether the delayed-gamma emission data are given as multigroup or discrete lines. To treat a discrete distribution, the integral in Eq. (5) is replaced by the sum (Bevington and Robinson, 1992)

$$r = \sum_{\tilde{x}=a}^{x} P(\tilde{x}), \tag{6}$$

where the variables are now discrete. Eq. (6) is then solved for x using a table-lookup scheme.

The following sections describe how Eq. (6) is evaluated in MCNPX for a given r so that x may be determined when $P(x)$ corresponds to energy or time CDFs for delayed-gamma emission.

4.2. Multigroup sampling.

In the following two subsections, the source and CDF for multigroup sampling are developed. The superscript "M" signifies "multigroup."

4.2.1. Source formulation.

The time- and energy-dependent delayed-gamma source calculated by MCNPX mimics nature. That is, the source of delayed gammas is simulated on a fission-event basis. The delayed-gamma source for each fission event is created by the decay of all fission products and their associated daughter products (Way and Wigner, 1948; Fisher and

Engle, 1964; Griffin, 1964). For each nuclide, the source is the product of the number of atoms of the nuclide, the probability that each atom will decay, and the probability that a decay will produce a photon of a given energy. The source contribution for the *i*th fission-product of interest, FP_i, and its decay products—a total of N_i nuclides for each *i*—can be written as

$$s_{i:n}^{M}(E,t) = N_{i:n}(t)\lambda_{i:n}p_{i:n}^{M}(E) \text{ (gammas/fission-s-MeV)}, \tag{7}$$

where $s_{i:n}^{M}(E,t)$ is the energy- and time-dependent number of delayed particles produced by nuclide *n* in the decay-chain associated with the ith fission product. In MCNPX, $i = 1,2$ for fission induced by sub-20-MeV neutrons and $i = 1,\ldots I$ for fission induced via the high-energy LAHET pathway. Additionally, $N_{i:n}(t)$ is the time-dependent nuclide atom density for the nth radioactive decay species associated with the ith fission product (atoms/fission), $\lambda_{i:n}$ is decay constant for FP_i and nuclide *n* (decay/atom-s), and $p_{i:n}^{M}(E)$ is the delayed-gamma production probability at energy *E* for FP_i and nuclide *n* (gammas/MeV-decay). Equation (7) corresponds to line 5, term 1 in Eq. (2) of Part III. The isotopic index "*i:p*" subscripting notation used in Eqs. (1)–(4) of Part III is altered to "*i:n*" in Eq. (7) (and in the following equations) to accentuate the association between the *i*th fission product and its decay progeny nuclides for neutron-induced fission (similar comments apply for the photofission-induced delayed terms given in Eqs.(1)–(4) of Part III).

Integration of the radionuclide-dependent delayed-gamma source, Eq. (7), over all energy and time gives the total number of delayed gammas emitted per fission for FP_i and each of its progeny n as

$$S_{i:n}^{M} = \int_0^\infty \int_0^\infty s_{i:n}^{M}(E,t)\,dE\,dt \text{ (gammas/fission).} \tag{8}$$

If this expression is summed over all n, the total source of delayed gammas for each FP_i chain is obtained as

$$S_{i}^{M} = \sum_{n=1}^{N_i} \int_0^\infty \int_0^\infty s_{i:n}^{M}(E,t)\,dE\,dt \text{ (gammas/fission).} \tag{9}$$

Summing this expression over all fission products then gives the total number of delayed particles due to emission over all time and energy due to all fission products and all of their progeny as

$$S^{M} = \sum_{i=1}^{I} \sum_{n=1}^{N_i} \int_0^\infty \int_0^\infty s_{i:n}^{M}(E,t)\,dE\,dt \text{ (gammas/fission).} \tag{10}$$

The expression for S^M is not available in analytic form because of the complexity of $N_{i:n}(t)$ that is embedded in $s_{i:n}^{M}(E,t)$. Thus, the integral expressions in Eqs. (8)–(10) must be evaluated approximately. To do so, Eq. (8) is written in the approximate finite-limit form

$$S_{i:n}^{M} \approx \sum_{j=1}^{J} \sum_{k=1}^{K} \int_{t_{j-1}}^{t_j} \int_{E_{k-1}}^{E_k} s_{i:n}^{M}(E,t)\,dE\,dt \text{ (gammas/fission).} \tag{11}$$

The average value of $s_{i:n}^{M}(E,t)$ for each time bin j and energy group k is

$$\overline{s}_{i:j,k,n}^{M} = \frac{\int_{t_{j-1}}^{t_j} \int_{E_{k-1}}^{E_k} s_{i:n}^{M}(E,t)\,dE\,dt}{\int_{t_{j-1}}^{t_j} \int_{E_{k-1}}^{E_k} dE\,dt} \text{ (gammas/fission-s-MeV).} \tag{12}$$

Inserting Eq. (7) into Eq. (12) gives

$$\overline{s}_{i:j,k,n}^{M} = \overline{N}_{i:j,n} \lambda_{i:n} \overline{p}_{i:k,n}^{M} \text{ (gammas/fission-s-MeV),} \tag{13}$$

where

$$\overline{N}_{i:j,n} = \frac{\int_{t_{j-1}}^{t_j} N_{i:n}(t)\,dt}{\Delta t_j} \text{ (atoms/fission),} \tag{14}$$

$$\Delta t_j = \int_{t_{j-1}}^{t_j} dt \text{ (s),} \tag{15}$$

$$\overline{p}_{i:k,n}^{M} = \frac{\int_{E_{k-1}}^{E_k} p_{i:n}^{M}(E)\,dE}{\Delta E_k} \text{ (gammas/MeV-decay),} \tag{16}$$

and

$$\Delta E_k = \int_{E_{k-1}}^{E_k} dE \text{ (MeV)}. \tag{17}$$

Here, for FP_i and each of its decay products n, $\overline{s}^{M}_{i:j,k,n}$ is the average number of delayed particles for time-bin j and energy-bin k, $\overline{N}_{i:j,n}$ is the time-bin average atom density (atoms/fission), $\lambda_{i:n}$ is the decay constant, and $\overline{p}^{M}_{i:k,n}$ is the energy-bin average delayed-gamma production probability (gammas/MeV-decay).

The $\overline{p}^{M}_{i:k,n}$ are evaluated as follows. The multigroup emission-data structure means that the data are confined to a series of bins $E_{k-1} < E \le E_k, k = 1, 2, ..., K$. Thus, the emission function may be characterized in a piecewise manner in terms of Heaviside functions. Thus,

$$p^{M}_{i:n}(E) = \sum_{k=1}^{K} H_1(E - E_{k-1}) H_2(E_k - E)\, p^{G}_{i:n}(E) \text{ (gammas/MeV-decay)}, \tag{18}$$

where $p^{G}_{i:n}(E)$ is a general emission function for the radionuclides and the Heaviside support is

$$\begin{aligned} H_1(E - E_{k-1}) &= \begin{Bmatrix} 0 & \text{for } E < E_{k-1} \\ 1 & \text{for } E \ge E_{k-1} \end{Bmatrix} \\ H_2(E_k - E) &= \begin{Bmatrix} 0 & \text{for } E_k < E \\ 1 & \text{for } E_k \ge E \end{Bmatrix} \end{aligned} \tag{19}$$

The integrated result

$$\int_0^\infty p_{i:n}^M(E)dE = \int_0^\infty \sum_{k=1}^K H_1(E-E_{k-1})H_2(E_k-E)\, p_{i:n}^G(E)dE$$
$$= \sum_{k=1}^K \int_{E_{k-1}}^{E_k} p_{i:k,n}^M(E)dE = \sum_{k=1}^K p_{i:k,n}^M \Delta E_k \quad \text{(gammas/decay)} \qquad (20)$$

is obtained, where

$$p_{i:k,n}^M(\mathrm{E}) = \left\{ \begin{matrix} p_{i:n}^G(E), & E_{k-1} < E \le E_k \\ 0, & \text{otherwise} \end{matrix} \right\} \text{(gammas/MeV-decay).} \qquad (21)$$

The final result in Eq. (20) stems from the fact that the emission function for the multigroup data is constant within each bin k. Thus, Eq. (16) becomes

$$\bar{p}_{i:k,n}^M = \frac{\int_{E_{k-1}}^{E_k} p_{i:n}^M(E)\,dE}{\Delta E_k} = \frac{p_{i:k,n}^M \Delta E_k}{\Delta E_k} = p_{i:k,n}^M \text{ (gammas/MeV-decay),} \qquad (22)$$

which is simply a statement that the average value of the emission probability in bin k is just the constant value in that bin.

Next, Eq. (13) is used as a means of obtaining an approximation to Eq. (11). Using Eqs. (16), (17), and (13), Eq. (12) may be rewritten as

$$\int_{t_{j-1}}^{t_j}\int_{E_{k-1}}^{E_k} s_{i:n}^{M}(E,t)\,dE\,dt = \bar{s}_{i:j,k,n}^{M}\Delta t_j \Delta E_k = (\bar{N}_{i:j,n}\lambda_{i:n}\bar{p}_{i:k,n}^{M})\Delta t_j \Delta E_k \quad \text{(gammas/fission).} \tag{23}$$

The time-averaged concentration $\bar{N}_{i:j,n}$ in time bin Δt_j can be approximated as follows. CINDER'90 calculates the analytic values of the atom densities $N_{i:j,n}$ for each FP_i and all of its daughter products n at the endpoints of each time bin $t_{j-1} < t \le t_j$ using its chain information and algorithms. Calculation of the exact time-averaged concentration $\bar{N}_{i:j,n}$ for $t_{j-1} < t \le t_j$ would require a detailed assessment of $N_{i:n}(t)$. Although CINDER'90 solves the chains analytically to provide concentrations at each bin boundary, the exact average value for each bin is not readily available. Instead, we use a trapezoidal rule approximation so that

$$\bar{N}_{i:j,n} = \frac{\int_{t_{j-1}}^{t_j} N_{i:n}(t)dt}{\int_{t_{j-1}}^{t_j} dt} \approx \frac{\int_{t_{j-1}}^{t_j} (N_{i:j-1,n} + m_{i:j,n}t)dt}{\Delta t_j} = \frac{N_{i:j-1,n} + N_{i:j,n}}{2} \quad \text{(atoms/fiss),} \tag{24}$$

where

$$m_{i:j,n} = \frac{N_{i:j,n} - N_{i:j-1,n}}{\Delta t_j} \quad \text{(gammas/fission-s).} \tag{25}$$

Using Eqs. (23) and (24), Eq. (11) becomes

$$S_{i:n}^{M} = \sum_{j=1}^{J}\sum_{k=1}^{K} \overline{s}_{i:j,k,n}^{M} \Delta t_j \Delta E_k = \sum_{j=1}^{J}\sum_{k=1}^{K} (\overline{N}_{i:j,n} \lambda_{i:n} \overline{p}_{i:k,n}^{M}) \Delta t_j \Delta E_k$$
$$= \sum_{j=1}^{J}\sum_{k=1}^{K} \left\{ \left[\frac{(N_{i:j-1,n} + N_{i:j,n})}{2} \right] \lambda_{i:n} \overline{p}_{i:k,n}^{M} \right\} \Delta t_j \Delta E_k \quad \text{(gammas/fission).} \tag{26}$$

Now let

$$\overline{P}_{i:k,n}^{M} = \overline{p}_{i:k,n}^{M} \Delta E_k \text{ (gammas/decay).} \tag{27}$$

The $\overline{P}_{i:k,n}^{M}$ are the emission-probability data contained in the CINDER'90 data file (cinder.dat). Computationally, CINDER'90 is called for each FP_i, and the data $N_{i:j,n}$ and $\lambda_{i:n}$ are returned. CINDER'90 sets $N_{n,j}$ to unity for each FP_i at $j = 0$ (and decays the FP_i to each j) and calculates the decay-product concentrations for each time t_j relative to this normalization. Then, using $N_{i:j,n}$, $\lambda_{i:n}$, and $\overline{P}_{i:k,n}^{M}$, the multigroup delayed source is constructed for each radionuclide.

Using Eq. (27), Eq. (26) becomes

$$S_{i:J,K,n}^{M} = \sum_{j=1}^{J}\sum_{k=1}^{K} \overline{N}_{i:j,n} \Delta t_j \lambda_{i:n} \overline{P}_{i:k,n}^{M} \text{ (gammas/fission).} \tag{28}$$

Then the summand in Eq. (28) is

$$S^{M}_{i:j,k,n} = \left[\frac{(N_{i:j-1,n} + N_{i:j,n})\Delta t_j}{2}\right]\lambda_{i:n}\overline{P}^{M}_{i:k,n} \text{ (gammas/fission).} \tag{29}$$

The source of delayed gammas emanating from the decay of a fission product and all of its radioactive daughters to time t_J is obtained by summing $S^{M}_{i:j,k,n}$ over all energies k and nuclides n to $j = JS \le J$ as

$$S^{M}_{i:JS,K} = \sum_{j=1}^{JS}\sum_{k=1}^{K}\sum_{n=1}^{N_i} S^{M}_{i:j,k,n} = \sum_{j=1}^{JS}\sum_{k=1}^{K}\sum_{n=1}^{N_i}\left[\frac{(N_{i:j-1,n} + N_{i:j,n})\Delta t_j}{2}\right]\lambda_{i:n}\overline{P}^{M}_{i:k,n} \text{ (gammas/fission),} \tag{30}$$

which may be rewritten as

$$\begin{aligned} S^{M}_{i:JS,K} &= \sum_{j=1}^{JS}\frac{\Delta t_j}{2}\sum_{k=1}^{K}\sum_{n=1}^{N_i}\left(N_{i:j-1,n} + N_{i:j,n}\right)\lambda_{i:n}\overline{P}^{M}_{i:k,n} \\ &= \sum_{j=1}^{JS}\frac{\Delta t_j}{2}\sum_{k=1}^{K}\sum_{n=1}^{N_i} N_{i:j-1,n}\lambda_{i:n}\overline{P}^{M}_{i:k,n} + \sum_{j=1}^{JS}\frac{\Delta t_j}{2}\sum_{k=1}^{K}\sum_{n=1}^{N_i} N_{i:j,n}\lambda_{i:n}\overline{P}^{M}_{i:k,n} \text{ (gammas/fission).} \\ &= \sum_{j=1}^{JS}\frac{\Delta t_j}{2}\sum_{k=1}^{K}\sum_{n=1}^{N_i}\tilde{S}^{M}_{i:j-1,k,n} + \sum_{j=1}^{JS}\frac{\Delta t_j}{2}\sum_{k=1}^{K}\sum_{n=1}^{N_i}\tilde{S}^{M}_{i:j,k,n} \\ &\equiv S^{M-T1}_{i:JS,K} + S^{M-T2}_{i:JS,K} \end{aligned} \tag{31}$$

The total delayed-gamma source for a fission event is obtained by adding the contributions from each radionuclide created by a fission event. This source includes each fission product and each of the radioactive decay products associated with each fission product. Thus, the $S^{M}_{i:JS,K}$ are summed over all I as

$$S^{M}_{JS,K} = \sum_{i=1}^{I} S^{M}_{i:JS,K} \text{ (gammas/fission)}, \tag{32}$$

where I is two for binary fission, or the number of residual nuclides from LAHET.

When $S^{M}_{JS,K}$ is evaluated for $JS = J$, the total number of delayed particles emitted for all time, $S^{M}_{J,K}$, or "S^{M}," is obtained as

$$S^{M} \equiv S^{M}_{J,K} \text{ (gammas/fission)}. \tag{33}$$

Equation (33) is Eq. (10) written in the form used in **CID**. This quantity is the total number of delayed particles emitted for a fission event. S^{M} is the factor used to normalize the emission distribution function in preparation for sampling.

An energy-dependent sampling distribution is still needed. If the sum in Eq. (30) is rearranged so that the outer sum involves the energy-bin index k, the sum in k is taken to $KS \le K$ and the sum in the time bin j is evaluated to $JS < J$, then

$$\begin{aligned} S^{M}_{i:JS,KS} &= \sum_{k=1}^{KS}\sum_{j=1}^{JS}\frac{\Delta t_j}{2}\sum_{n=1}^{N_i}(N_{i:j-1,n} + N_{i:j,n})\lambda_{i:n}\overline{P}^{M}_{i:k,n} \\ &= \sum_{k=1}^{KS}\sum_{j=1}^{JS}\frac{\Delta t_j}{2}\sum_{n=1}^{N_i}N_{i:j-1,n}\lambda_{i:n}\overline{P}^{M}_{i:k,n} + \sum_{k=1}^{KS}\sum_{j=1}^{JS}\frac{\Delta t_j}{2}\sum_{n=1}^{N_i}N_{i:j,n}\lambda_{i:n}\overline{P}^{M}_{i:k,n} \text{ (gammas/fission).} \\ &= \sum_{k=1}^{KS}\sum_{j=1}^{JS}\frac{\Delta t_j}{2}\tilde{S}^{M}_{i:j-1,k} + \sum_{k=1}^{KS}\sum_{j=1}^{JS}\frac{\Delta t_j}{2}\tilde{S}^{M}_{i:j,k} \end{aligned} \tag{34}$$

In MCNPX, the FP_i is determined in **CID** for each product created by a fission event (as discussed in Section 2, this number is either two for binary fission or the number of residual nuclides passed by LAHET). **CID** then calls **cid_sampf1**, wherein the $S^M_{i:JS,KS}$ are calculated for each FP_i and, as Eq. (34) indicates, all of the decay products N_i associated with the FP_i, as well as for each (integrated) delay time (index) *JS* and emission energy (index) *KS*. Further discussion regarding the computational implications of the $S^M_{i:JS,KS}$ is presented in Section 4.5. As is seen in the following section, $S^M_{J,KS}$ — i.e., $S^M_{i:JS,KS}$ summed over all *i*—are used to form the delayed-gamma cumulative distribution function for a fission event.

4.2.2. Multigroup emission-energy sampling.

Sampling distributions may now be obtained. First, Eq. (7) is divided by S^M to give the delayed-gamma emission probability for FP_i and its associated *n* radioactive decay daughters $\chi^M_{i:n}(E,t)$ as

$$\chi^M_{i:n}(E,t) = \frac{s^M_{i:n}(E,t)}{S^M} \text{ (/MeV-s).} \tag{35}$$

Summation over all *i* and *n* gives the total delayed-gamma emission probability as a function of time and energy as

$$\chi^M(E,t) = \sum_{i=1}^{I}\sum_{n=1}^{N_i} \chi_{i:n}^M(E,t) = \sum_{i=1}^{I}\sum_{n=1}^{N_i} \frac{s_{i:n}^M(E,t)}{S^M} \text{ (/MeV-s).} \tag{36}$$

For the purposes of normalization, with Eq. (8),

$$\begin{aligned}\int_0^\infty \int_0^\infty \chi^M(E,t)\,dEdt &= \int_0^\infty \int_0^\infty \sum_{i=1}^{I}\sum_{n=1}^{N_i} \chi_{i:n}^M(E,t)\,dEdt \\ &= \int_0^\infty \int_0^\infty \sum_{i=1}^{I}\sum_{n=1}^{N_i} \frac{s_{i:n}^M(E,t)}{S^M} dEdt = 1\end{aligned} \tag{37}$$

If the integrals in Eq. (37) are terminated at finite limits, then

$$\begin{aligned}\Xi_{J,K}^M &= \int_0^{t_J} \int_0^{E_K} \sum_{i=1}^{I}\sum_{n=1}^{N_i} \chi_{i:n}^M(E,t)\,dEdt = \int_0^{t_J} \int_0^{E_K} \sum_{i=1}^{I}\sum_{n=1}^{N_i} \frac{s_{i:n}^M(E,t)}{S^M} dEdt \\ &= \frac{1}{S^M} \sum_{i=1}^{I}\sum_{n=1}^{N_i}\sum_{j=1}^{J}\sum_{k=1}^{K} \int_{t_{j-1}}^{t_j} \int_{E_{k-1}}^{E_k} s_{i:n}^M(E,t)\,dEdt\end{aligned} \tag{38}$$

By Eq. (23), this equation reduces to

$$\Xi_{J,K}^M = \int_0^{t_J} \int_0^{E_K} \sum_{i=1}^{I}\sum_{n=1}^{N_i} \chi_{i:n}^M(E,t)\,dEdt = \frac{1}{S^M} \sum_{i=1}^{I}\sum_{n=1}^{N_i}\sum_{j=1}^{J}\sum_{k=1}^{K} \overline{s}_{i:j,k,n}^M \Delta t_j \Delta E_k\,. \tag{39}$$

The summand of Eq. (39) may be written as

$$\chi_{i:j,k,n}^M = \frac{\overline{s}_{i:j,k,n}^M}{S^M} \Delta t_j \Delta E_k \text{ (/MeV-s).} \tag{40}$$

Inserting Eq. (13) into Eq. (39) and using Eqs. (24) and (27) give

$$\Xi_{J,K}^{M} = \int_0^{t_J} \int_0^{E_K} \sum_{i=1}^{I} \sum_{n=1}^{N_i} \chi_{i:n}^{M}(E,t)\, dEdt$$
$$= \frac{1}{S^M} \sum_{i=1}^{I} \sum_{n=1}^{N_i} \sum_{j=1}^{J} \sum_{k=1}^{K} \left[\frac{(N_{i:n,j-1} + N_{i:n,j})\Delta t_j}{2} \right] \lambda_{i:n} \overline{P}_{i:k,n}^{M} \quad . \tag{41}$$

By Eq. (29), the summand in Eq. (41) is

$$\Xi_{i:j,k,n}^{M} = \frac{S_{i:j,k,n}^{M}}{S^M} \quad . \tag{42}$$

At this point, the derivation contained in Eqs.(30)–(34) may be used to obtain

$$\Xi_{J,KS}^{M} = \frac{1}{S^M} \sum_{k=1}^{KS} \sum_{i=1}^{I} \sum_{j=1}^{J} \frac{\Delta t_j}{2} \sum_{n=1}^{N_i} (N_{i:j-1,n} + N_{i:j,n}) \lambda_{i:n} \overline{P}_{i:k,n}^{M} = \frac{S_{J,KS}^{M}}{S^M} \, . \tag{43}$$

$\Xi_{J,KS}^{M}$ is the cumulative distribution function that is used to sample delayed-gamma emission as a function of energy. This CDF is formed by including the gamma rays emitted by each FP_i and each of its N_i associated radioactive decay products. The notation $\Xi_{J,KS}^{M}$ signifies summation (i.e., integration) over energy (versus $\Xi_{JS,k}^{M}$, which is the kth term). Also, $\Xi_{J,K}^{M}$=1, i.e., the integrated CDF is unity due to its normalization. Equation (43) is the equivalent of the general statistical result of Eq. (5). If the upper time and energy limits were infinity, then the result would include the entire delayed source. However, in practice, these limits are finite. Therefore, a portion of the total delayed source will be omitted.

To understand the computational evaluation of Eq. (43), the discussion in Section 4.5.2 indicates that if a random number r_e is selected by the toss of a uniform random number generator of the form of Eq. (1), then the sum

$$r_q = \Xi^M_{q,KS} \tag{44}$$

can be evaluated for q terms until the indices $q = l$ and $q = h$ are identified so that $\Xi^M_{l,KS} < r_q < \Xi^M_{h,KS}$ and, as a result of the use of known energies E_k to calculate the $\Xi^M_{q,KS}$, the E_{dl} and E_{dh}. Because the treatment is discretized, the precise value E_e corresponding to r_e will not usually be found. To accommodate this imprecision, the emission energy E_e is randomly estimated on the interval $E_{dl} < E_e < E_{dh}$. Thus, the multigroup delayed-gamma emission energy is random within an energy bin.

4.2.3. Multigroup emission-time sampling.

If the sums involving energy and time contained in Eq. (43) are done so that the energy sum extends over all energies and the time sum is extended to each time-bin limit, then a CDF in time is obtained as

$$\Xi^M_{JS,K} = \frac{1}{S^M}\sum_{k=1}^{K}\sum_{i=1}^{I}\sum_{j=1}^{JS}\frac{\Delta t_j}{2}\sum_{n=1}^{N_i}(N_{i;j-1,n} + N_{i;j,n})\lambda_{i;n}\overline{P}^M_{i;k,n} = \frac{S^M_{JS,K}}{S^M}. \tag{45}$$

The numerator is recognized as the aggregate number of particles emitted to the end of time-bin j.

From Eq.(43), we know only that emission has been done by random sampling within an energy bin. The identity of the emitting nuclide cannot be determined. Thus, time-based emission is done using the aggregate decay characteristics of the fission or residual event rather the emitting nuclide.

4.3. Line sampling.

The derivations in the following two subsections address the treatment of line delayed-gamma source data. The superscript "L" is used to connote line data.

4.3.1. Source formulation.

The time- and energy-dependent source of delayed particles is created by the decay of all fission products and their daughter products. The source contribution for the $\tilde{i}^{\text{th}}$ fission-product of interest, $\text{FP}_{\tilde{i}}$, and its decay products for each $\tilde{i}$ —$N_{\tilde{i}}$ total nuclides—can be written as

$$s^{L}_{\tilde{i}:\tilde{n}}(E,t) = N_{\tilde{i}:\tilde{n}}(t)\lambda_{\tilde{i}:\tilde{n}}\, p^{L}_{\tilde{i}:\tilde{n}}(E) \text{ (gammas/fission-s-MeV)}, \tag{46}$$

where $s_{\tilde{i}:\tilde{n}}(E,t)$ is the energy- and time-dependent number of delayed particles produced by nuclide $\tilde{n}$, $N_{\tilde{i}:\tilde{n}}(t)$ is the time-dependent nuclide atom density for the $\tilde{n}^{\text{th}}$ radioactive

decay species associated with the $\tilde{i}^{\text{th}}$ fission product (atoms/fiss), $\lambda_{\tilde{i}:\tilde{n}}$ is decay constant for $\text{FP}_{\tilde{i}}$ and nuclide $\tilde{n}$ (decay/atom-s), and $p^{L}_{\tilde{i}:\tilde{n}}(E)$ is the delayed-gamma production probability at energy E for $\text{FP}_{\tilde{i}}$ and nuclide $\tilde{n}$ (gammas/MeV-decay).

Integration of Eq. (46) over all energy and time gives the total number of delayed gammas emitted per fission for $\tilde{i}$ and $\tilde{n}$ due to line emission as

$$S^{L}_{\tilde{i}:\tilde{n}} = \int_0^{\infty}\int_0^{\infty} s^{L}_{\tilde{i}:\tilde{n}}(E,t)\,dE\,dt \quad \text{(gammas/fission).} \tag{47}$$

The line data are represented as a series of values at discrete energies. Thus, the line sources are conveniently represented using Kronecker delta functions so that

$$p^{L}_{\tilde{i}:\tilde{n}}(E) = \sum_{\tilde{k}=1}^{\tilde{K}} \delta(E_{\tilde{k}})\, p^{G}_{\tilde{i}:\tilde{n}}(E) \quad \text{(gammas/MeV-decay),} \tag{48}$$

where the Kronecker delta is

$$\delta_{\tilde{k}} = \begin{Bmatrix} 0 & \text{for } E \neq E_{\tilde{k}} \\ 1 & \text{for } E = E_{\tilde{k}} \end{Bmatrix}, \tag{49}$$

$p^{G}_{\tilde{i}:\tilde{n}}(E)$ is the general nuclide emission function, and $\tilde{K}$ is the total number of lines. As was discussed in Section 3, the cindergl.dat data also include so-called continuous contribution for many nuclides. The continuous data are differential data; thus, they are

integrated (over their 10-keV bin structure) before being included for use in addition to the discrete-emission data.

Inserting Eq. (48) into Eq. (46) and inserting the result into Eq. (47) gives, after integrating over energy,

$$\begin{aligned} S^{L}_{\bar{i}:\bar{n}} &= \int_0^\infty N_{\bar{i}:\bar{n}}(t)\lambda_{\bar{i}:\bar{n}} \sum_{\bar{k}=1}^{\bar{K}} p^{L}_{\bar{i}:\bar{k},\bar{n}} dt \\ &= \int_0^\infty \sum_{\bar{k}=1}^{\bar{K}} N_{\bar{i}:\bar{n}}(t)\lambda_{\bar{i}:\bar{n}} p^{L}_{\bar{i}:\bar{k},\bar{n}} dt \end{aligned} \quad \text{(gammas/fission)}, \tag{50}$$

where

$$p^{L}_{\bar{i}:\bar{k},\bar{n}} = p^{G}_{\bar{i}:\bar{n}}(E_{\bar{k}}) \,. \tag{51}$$

Use of the results of Eqs. (14) and (15) with line-emission subscripts gives

$$S^{L}_{\bar{i}:J,\bar{K},\bar{n}} = \sum_{j=1}^{J} \sum_{\bar{k}=1}^{\bar{K}} \bar{N}_{\bar{i}:j,\bar{n}} \Delta t_j \lambda_{\bar{i}:\bar{n}} p^{L}_{\bar{i}:\bar{k},\bar{n}} \quad \text{(gammas/fission)}. \tag{52}$$

Equation (52) closely resembles the multigroup-data result of Eq. (28), with the difference stemming from the summation for bins and lines, respectively.

Following the development in Eq. (24), the summand in Eq. (52) can be rewritten as

$$S^{L}_{\tilde{i}:j,\tilde{k},\tilde{n}} = \left[\frac{(N_{i:j-1,n} + N_{i:j,n})\Delta t_j}{2}\right]\lambda_{\tilde{i}:\tilde{n}} p^{L}_{\tilde{i}:\tilde{k},\tilde{n}} \text{ (gammas/fission)}, \tag{53}$$

which is the delayed-gamma source for each radionuclide during time bin j. The sum of $S^{L}_{\tilde{i}:j,\tilde{k},\tilde{n}}$ over all j, $\tilde{k}$, and $\tilde{n}$ is

$$S^{L}_{\tilde{i}:JS,\tilde{K}} = \sum_{j=1}^{JS}\sum_{\tilde{k}=1}^{\tilde{K}}\sum_{\tilde{n}=1}^{\tilde{N}\tilde{i}} S^{L}_{\tilde{i}:j,\tilde{k},\tilde{n}} = \sum_{j=1}^{JS}\sum_{\tilde{k}=1}^{\tilde{K}}\sum_{\tilde{n}=1}^{\tilde{N}\tilde{i}}\left[\frac{(N_{\tilde{i}:j-1,\tilde{n}} + N_{\tilde{i}:j,\tilde{n}})\Delta t_j}{2}\right]\lambda_{\tilde{i}:\tilde{n}} p^{L}_{\tilde{i}:\tilde{k},\tilde{n}} \text{ (gammas/fission)}, \tag{54}$$

which may be rewritten as

$$\begin{aligned}
S^{L}_{\tilde{i}:JS,\tilde{K}} &= \sum_{j=1}^{JS}\frac{\Delta t_j}{2}\sum_{\tilde{k}=1}^{\tilde{K}}\sum_{\tilde{n}=1}^{\tilde{N}\tilde{i}}\left(N_{\tilde{i}:j-1,\tilde{n}} + N_{\tilde{i}:j,\tilde{n}}\right)\lambda_{\tilde{i}:\tilde{n}} p^{L}_{\tilde{i}:\tilde{k},\tilde{n}} \\
&= \sum_{j=1}^{JS}\frac{\Delta t_j}{2}\sum_{\tilde{k}=1}^{\tilde{K}}\sum_{\tilde{n}=1}^{\tilde{N}\tilde{i}} N_{\tilde{i}:j-1,\tilde{n}}\lambda_{\tilde{i}:\tilde{n}} p^{L}_{\tilde{i}:\tilde{k},\tilde{n}} + \sum_{j=1}^{JS}\frac{\Delta t_j}{2}\sum_{\tilde{k}=1}^{\tilde{K}}\sum_{\tilde{n}=1}^{\tilde{N}\tilde{i}} N_{\tilde{i}:j,\tilde{n}}\lambda_{\tilde{i}:\tilde{n}} p^{L}_{\tilde{i}:\tilde{k},\tilde{n}} \text{ (gammas/fission)}. \\
&= \sum_{j=1}^{JS}\frac{\Delta t_j}{2}\sum_{\tilde{k}=1}^{\tilde{K}}\sum_{\tilde{n}=1}^{\tilde{N}\tilde{i}} \tilde{S}^{L}_{\tilde{i}:j-1,\tilde{k},\tilde{n}} + \sum_{j=1}^{JS}\frac{\Delta t_j}{2}\sum_{\tilde{k}=1}^{\tilde{K}}\sum_{\tilde{n}=1}^{\tilde{N}\tilde{i}} \tilde{S}^{L}_{\tilde{i}:j,\tilde{k},\tilde{n}} \\
&\equiv S^{L-T1}_{\tilde{i}:JS,\tilde{K}} + S^{L-T2}_{\tilde{i}:JS,\tilde{K}}.
\end{aligned} \tag{55}$$

The $S^{L}_{\tilde{i}:JS,\tilde{K}}$ may be summed over all $\tilde{i}$ as

$$S^{L}_{JS,\tilde{K}} = \sum_{\tilde{i}=1}^{\tilde{I}} S^{L}_{\tilde{i}:JS,\tilde{K}} \text{ (gammas/fission)}, \tag{56}$$

where $\tilde{I}$ is two for fission and is the number of residual nuclides for high-energy (LAHET) interactions. S^{L}_{JS} represents the total number of delayed particles emitted by all

radionuclides by the end of time bin j. When evaluated for $j = J$, $S^L_{J,\tilde{K}}$, or "S^L," is the total number of delayed particles emitted in the form of lines for all time, as

$$S^L \equiv S^L_{J,\tilde{K}} \text{ (gammas/fission).} \tag{57}$$

S^L is the factor used to normalize the line-emission distribution function in preparation for sampling.

Rearranging the sum in Eq. (54) forms the energy-dependent portion of the sampling distribution. The outer sum thus involves the energy-bin index $\tilde{k}$, and the sum in the time-bin j is evaluated to $JS < J$ so that

$$\begin{aligned} S^L_{\tilde{i}:JS,\tilde{K}S} &= \sum_{\tilde{k}=1}^{\tilde{K}S}\sum_{j=1}^{JS}\frac{\Delta t_j}{2}\sum_{\tilde{n}=1}^{\tilde{N}\tilde{i}}(N_{\tilde{i}:j-1,\tilde{n}} + N_{\tilde{i}:j,\tilde{n}})\lambda_{\tilde{i}:\tilde{n}}p^L_{\tilde{i}:k,\tilde{k},\tilde{n}} \\ &= \sum_{\tilde{k}=1}^{\tilde{K}S}\sum_{j=1}^{JS}\frac{\Delta t_j}{2}\sum_{\tilde{n}=1}^{\tilde{N}\tilde{i}}N_{\tilde{i}:j-1,\tilde{n}}\lambda_{\tilde{i}:\tilde{n}}p^L_{\tilde{i}:\tilde{k},\tilde{n}} + \sum_{\tilde{k}=1}^{\tilde{K}S}\sum_{j=1}^{JS}\frac{\Delta t_j}{2}\sum_{n=1}^{\tilde{N}\tilde{i}}N_{\tilde{i}:j,\tilde{n}}\lambda_{\tilde{i}:\tilde{n}}p^L_{\tilde{i}:\tilde{k},\tilde{n}} \text{ (gammas/fission).} \\ &= \sum_{\tilde{k}=1}^{\tilde{K}S}\sum_{j=1}^{JS}\frac{\Delta t_j}{2}\tilde{S}_{\tilde{i}:j-1,\tilde{k}} + \sum_{\tilde{k}=1}^{\tilde{K}S}\sum_{j=1}^{JS}\frac{\Delta t_j}{2}\tilde{S}_{\tilde{i}:j,\tilde{k}} \end{aligned} \tag{58}$$

If $S^L_{\tilde{i}}$ is summed over all $\mathrm{FP}_{\tilde{i}}$, then the total number of delayed gammas per fission S^L emitted over all energies, times, and radioactive products is obtained. In a manner paralleling that for multigroup treatment, $S^L_{J,\tilde{K}S}$ will be used to form the delayed-gamma cumulative distribution function for line-data radionuclides.

4.3.2. Line emission-energy sampling.

The line-emission sampling distributions may now be obtained. First, Eq. (46) is divided by S^L to give the delayed-gamma emission probability for $\mathrm{FP}_{\tilde{i}}$ and its associated radioactive decay daughters, $\chi^{D-L}_{\tilde{i}:\tilde{n}}(E,t)$, as

$$\chi^{L}_{\tilde{i}:\tilde{n}}(E,t) = \frac{s^{L}_{\tilde{i}:\tilde{n}}(E,t)}{S^L} \text{ (/MeV-s).} \tag{59}$$

Summation over all $\tilde{i}$ and $\tilde{n}$ gives the total delayed-gamma emission probability as a function of time and energy as

$$\chi^{L}(E,t) = \sum_{\tilde{i}=1}^{\tilde{I}} \sum_{\tilde{n}=1}^{\tilde{N}\tilde{i}} \chi^{L}_{\tilde{i}:\tilde{n}}(E,t) = \sum_{\tilde{i}=1}^{\tilde{I}} \sum_{\tilde{n}=1}^{\tilde{N}\tilde{i}} \frac{s^{L}_{\tilde{i}:\tilde{n}}(E,t)}{S^L} \text{ (s}^{-1}\text{)} \tag{60}$$

which, when integrated over all time and energy, yields a result of unity. Then, following the derivation used for multigroup data,

$$\Xi^{L}_{J,\tilde{K}S} = \frac{1}{S^L} \sum_{\tilde{k}=1}^{\tilde{K}S} \sum_{\tilde{i}=1}^{\tilde{I}} \sum_{j=1}^{J} \frac{\Delta t_j}{2} \sum_{n=1}^{\tilde{N}\tilde{i}} (N_{\tilde{i}:j-1,\tilde{n}} + N_{\tilde{i}:j,\tilde{n}}) \lambda_{\tilde{i}:\tilde{n}} p^{L}_{\tilde{i}:\tilde{k},\tilde{n}} = \frac{S^{L}_{J,\tilde{K}S}}{S^L} \tag{61}$$

is obtained. $\Xi^{L}_{J,\tilde{K}S}$ is the delayed-gamma cumulative distribution function that is used to sample delayed-gamma line emission as a function of energy.

4.3.3. Emission-time sampling.

For line-based emission, the identity of the emitting nuclide is known. Thus, time-based emission is done based on the emission probability for the emitting nuclide. In general, the emission probability for a line-emitting nuclide with atom density $N_{\tilde{i}:\tilde{n}}(t)$ is given by

$$\Xi_{\tilde{i},\tilde{n}}^{D-L}(\tau) = \int_0^{\tau} C_{\tilde{i}:\tilde{n}} N_{\tilde{i}:\tilde{n}}(t)dt = r\,, \tag{62}$$

where $C_{\tilde{i}:\tilde{n}}$ is a normalization constant for the time CDF and r is a pseudo-random number on the interval [0,1].

For a principal fission product or residual,[†] the time emission can be expressed analytically. The time-dependent atom density is simply exponential in behavior and $C_{\tilde{i}:\tilde{n}} = \lambda_{\tilde{i},\tilde{n}}$ with $\tilde{n} = 1$ and $\tilde{i} = 1$ or 2, depending on whether the fission product is the first or second sample. In this case, sampling for the emission time is given by (Bevington and Robinson, 1992, pp 90–91)

$$\tau = -\log(r) / \lambda_{\tilde{i}:\tilde{n}}\,. \tag{63}$$

This expression gives the precise emission time for the delayed gamma.

For a nuclide that is created due to the radioactive decay product of one or more of its precursors, the emission-time sampling must reflect the decay of each of its precursors. From Eq.(24), the integral in Eq.(62) can be approximated using the trapezoidal rule in terms of time-dependent atom densities at times t_{j-1} and t_j. Using these atom densities, and evaluating the normalization condition

[†] The parent species in a decay chain.

$$\int_0^\infty C_{\tilde{i}:\tilde{n}} N_{\tilde{i}:\tilde{n}}(t)dt = 1 \tag{64}$$

for $C_{\tilde{i}:\tilde{n}}$ yields the time-CDF expression

$$\Xi^{D-L}_{\tilde{i},JS,\tilde{n}} = \frac{\sum_{j=1}^{JS} \Delta t_j (N_{\tilde{i}:j-1,\tilde{n}} + N_{\tilde{i}:j,\tilde{n}})}{\sum_{j=1}^{J} \Delta t_j (N_{\tilde{i}:j-1,\tilde{n}} + N_{\tilde{i}:j,\tilde{n}})} = r\,. \tag{65}$$

The requisite atom-density data for Eq.(65) are calculated by CINDER'90 at a set of J times. Equation (65) is evaluated for a given random number by table lookup (i.e., stepping in the time index j until the expression at $j-1$ and j bounds r). A second random number is then tossed to randomly select the emission time between times t_{j-1} and t_j. Thus, for a non-principal nuclide, the emission time is approximated in a time interval.

4.4. Mixed multigroup and line sampling.

Finally, consideration is given to the case in which a mixture of multigroup and line data exists. The source is thus

$$S = S^M + S^L \text{ (gammas/fission).} \tag{66}$$

4.4.1. Emission-energy sampling.

The energy-, time-, and nuclide-dependent chi is

$$\chi^{ML}_{i:n;\tilde{i},\tilde{n}}(E,t) = \frac{s^M_{i:n}(E,t) + s^L_{\tilde{i}:\tilde{n}}(E,t)}{S} \quad . \tag{67}$$

The energy- and time-dependent chi is obtained by summing over all multigroup and line nuclides as

$$\chi^{ML}(E,t) = \frac{\sum_{i=1}^{I}\sum_{n=1}^{N_i} s^M_{i:n}(E,t) + \sum_{\tilde{i}=1}^{\tilde{I}}\sum_{\tilde{n}=1}^{\tilde{N}\tilde{i}} s^L_{\tilde{i}:\tilde{n}}(E,t)}{S} \quad . \tag{68}$$

By Eqs. (8), (47), and (66), the integral of $\chi^{ML}(E,t)$ over all time and energy is unity. If finite limits in time and energy are used for the integral of Eq. (68), then the CDF in time (t_J) and energy (E_K for multigroup and $E_{\tilde{K}}$ for lines) is obtained as

$$\Xi^{ML}_{J,K} = \frac{1}{S}\int_0^{t_J}\int_0^{E_K}\sum_{i=1}^{I}\sum_{n=1}^{N_i} s^M_{i:n}(E,t)dEdt + \frac{1}{S}\int_0^{t_J}\int_0^{E_{\tilde{K}}}\sum_{\tilde{i}=1}^{\tilde{I}}\sum_{\tilde{n}=1}^{\tilde{N}\tilde{i}} s^L_{\tilde{i}:\tilde{n}}(E,t)dEdt \; . \tag{69}$$

Breaking the integrals in time and energy into intervals, using Eqs. (23) and (52), and rearranging the summation order gives

$$\begin{aligned}\Xi^{ML}_{J,KS,\tilde{K}S} &= \frac{1}{S}\sum_{k=1}^{KS}\sum_{i=1}^{I}\sum_{j=1}^{J}\frac{\Delta t_j}{2}\sum_{n=1}^{N_i}\left(N_{i:j-1,n} + N_{i:j,n}\right)\lambda_{i:n}\overline{P}^M_{i:k,n} \\ &\quad + \frac{1}{S}\sum_{\tilde{k}=1}^{\tilde{K}S}\sum_{\tilde{i}=1}^{\tilde{I}}\sum_{j=1}^{J}\frac{\Delta t_j}{2}\sum_{\tilde{n}=1}^{\tilde{N}\tilde{i}}(N_{\tilde{i}:j-1,\tilde{n}} + N_{\tilde{i}:j,\tilde{n}})\lambda_{\tilde{i}:\tilde{n}}p^L_{\tilde{i}:\tilde{k},\tilde{n}} \quad . \\ &= \frac{S^M_{J,KS} + S^L_{J,\tilde{K}S}}{S}\end{aligned} \tag{70}$$

The difference in energy boundaries in Eq. (70) for the multigroup and line components must be reconciled for computational evaluation. Breaking the multigroup contribution into pieces such that its energy boundaries coincide with the energies of the lines affects the reconciliation. Thus,

$$
\begin{aligned}
\Xi^{ML}_{J,\tilde{K}S} &= \frac{1}{S}\sum_{\tilde{k}=1}^{\tilde{K}S}\sum_{i=1}^{I}\sum_{j=1}^{J}\frac{\Delta t_j}{2}\sum_{n=1}^{N_i}\left(N_{i,j-1,n}+N_{i:j,n}\right)\lambda_{i:n}\sum_{k=1}^{K_{\tilde{k}}}\overline{P}^{M}_{i:\tilde{k},k,n}\frac{\Delta E_{\tilde{k}}}{\Delta E_k} \\
&\quad + \frac{1}{S}\sum_{\tilde{k}=1}^{\tilde{K}S}\sum_{\tilde{i}=1}^{\tilde{I}}\sum_{j=1}^{J}\frac{\Delta t_j}{2}\sum_{\tilde{n}=1}^{\tilde{N}\tilde{i}}(N_{\tilde{i}:j-1,\tilde{n}}+N_{\tilde{i}:j,\tilde{n}})\lambda_{\tilde{i}:\tilde{n}}p^{L}_{\tilde{i}:\tilde{k},\tilde{n}} \\
&= \frac{S^{M}_{J,\tilde{K}S}+S^{L}_{J,\tilde{K}S}}{S} \\
&= \Xi^{ML-M}_{J,\tilde{K}S}+\Xi^{ML-L}_{J,\tilde{K}S}
\end{aligned}
\tag{71}
$$

$\Xi^{ML}_{J,\tilde{K}S}$ is the CDF for delayed-gamma emission-energy sampling for a set of nuclides where the emission spectra are characterized by a combination of multigroup and line data. This CDF is formed by including the gamma rays emitted by each fission product created by a fission event, along with each of its associated radioactive decay products. The CDF includes radionuclides where the emission-spectra data are either multigroup or line.

For computational application, consider a model in which some of the radionuclides are emitting photons in an energy range $E_{k-1} < E \le E_k$ based on multigroup emission-probability data, whereas other radionuclides are emitting photons in the identical energy range via a line-emission characterization. It is evident that the sampling process for this

energy range will involve determining whether a particular photon is emitted by the multigroup or line set of radionuclides. If the emission is based on multigroup data, then the emission energy is randomly selected in bin k because the photons can be emitted at any energy within a bin. If it is determined that a line-set radionuclide is the emitter, then the specific energy of the line closest to the randomly generated energy is selected (using **FIND_GAMMAL**) because the photons are emitted only at discrete energies.

Note how the desired limits are obtained if the data comprise either all multigroup or line data. This expression shows precisely how to calculate this CDF—the contribution for line data is obtained in the manner used for multigroup data, with the addition of a loop on $\tilde{k}$ to sum the contribution of all lines within energy bin k. The sum in the energy-bin variable k is evaluated to $KS \leq K$, which is the discretized approximation to the integral in energy from zero to energy E_k.

4.4.2. Emission-time sampling.

For a fission or residual event, if multigroup emission is selected, then Eq.(45) is used to sample the emission time. If line emission is selected, then either Eq.(63) (principal residual) or Eq.(65) (decay-chain nuclide) is used.

4.4.3. Number of delayed gammas emitted.

The number of delayed gammas emitted per fission event is determined by randomly sampling the total number of delayed gammas calculated by Eq. (66). This number can range from zero to the integer value of S.

4.5. Computational sampling.

The development presented in Sections 4.2–4.4 is reviewed in this section for deployment as a practical computing algorithm in MCNPX. This discussion includes some of the issues associated with competition between storage and execution issues and presents some techniques that have been developed to manage these issues. Additionally, the algorithmic recipe used in MCNPX is described.

4.5.1. Practical computational sampling.

In principle, the sampling processes detailed in Sections 4.2–4.4 can be performed for all radionuclides using a large number of integration times and the exact energies of the emission lines so as to obtain high-fidelity emission as a function of time and energy. However, such fidelity comes at a price due to several key factors, including (1) the calculation of atom densities, (2) the quantity of emission data, (3) the calculation of the CDFs, and (4) storage limitations.

The CDFs are formed at a series of discrete times. The required atom densities must be calculated using CINDER'90 at each desired emission time. Our testing has led us to use a set of approximately 100 time values, ranging from 1×10^{-7} to 10^{9} s. The values provide

a reasonable coverage of the bulk of emission times of interest for a variety of applications.†

The CDFs are formed for a series of discrete energies or energy bins. As noted in Table 1, there are over 280,000 emission data for 979 nuclides. All other nuclides are treated using 25-group data. The CDFs are formed for pairs of fission products (or for individual residual nuclides) and their decay progeny. Some radioactive species have few emission data, whereas others can have hundreds of such data. Consequently, there can be tens to thousands of emission energies associated with each CDF. The quantity of emission data causes time-consuming and storage-intensive operations.

The CDF given by Eq.(71) contains nested sums involving time, energy, and nuclide indices. The act of calculating these sums for each fission or activation event is in itself time consuming.

These factors cause execution and storage penalties. As such, the code user may desire to execute lower-fidelity results wherein only portions of data are treated, or they are treated in a coarse manner. Alternatively, a user may wish to execute high-fidelity simulations, but encounter storage issues that can arise even though many modern computing systems have 1 GB or more of RAM.

† At present, these data are "hard-wired" into the code in the "d" array in subroutine CID. A future update may be implemented to enable the user to specify values.

Competing with the storage-limitation issue are the relatively time consuming CINDER'90 calculations (for atom densities) and the CDF-creation calculations. It is essential that repetitive calculations are minimized or eliminated by storing and reusing CDF data whenever dynamically allocatable memory is available.

The greatest storage demand (by far) for the delayed-gamma MCNPX feature is associated with the source values $S^{M}_{i:JS,KS}$ and $S^{L}_{\tilde{i}:JS,\tilde{K}S}$ given in Eqs. (34) and (58) for multigroup and line data, respectively. In principle, these values can (and should) be calculated once for each fission product i because a particular fission product and its decay products will be invariant as a function of fission event. Each such calculation includes a call to CINDER'90 for the requisite data. The $S^{M}_{i:JS,KS}$ and $S^{L}_{\tilde{i}:JS,\tilde{K}S}$ can then be saved for reuse, thereby eliminating repetitive (expensive) calls to CINDER'90 and the recalculation of these values. Indeed, in MCNPX, these values are stored in arrays named **gg2** and **gg2_l**.

The difficulty with this strategy is the array-storage demands. As the subscripts for these sources indicate, these arrays involve the number of species, the number of delay times, and the number of energies. If we refer to Eqs. (34) and (58), the energy index depends on the number of emission energies for a fission product plus those for all of its decay products. Typical values for three indices are thus thousands, tens to hundreds, and tens to thousands, respectively.

In an attempt to satisfy the competing storage and execution-speed constraints, several control techniques have been developed. These techniques revolve around the use and treatment of line data.

One such technique involves evaluating the CDF energy integrals using either binwise or line-by-line treatments. Binwise integration involves the use of integration limits that coincide with the 25-group cinder.dat structure. The line-data CDF integral is thus calculated by lumping all lines into the multigroup energy structure. Simulation tests suggest that the default energy integration scheme provides reliable coarse-fidelity results (see the results for the Fisher and Engle experiment presented in Section 2.1 of Part II) with reasonable/reduced computing times, and is deployable on personal computers.

High-fidelity delayed-gamma emission spectra can be calculated using line-by-line ("exact") integration. The integration limits (for the lines and multigroup data) are taken to be either the midpoint energies between adjacent lines, or a multigroup boundary. As such, for exact integration, the integration limits are dependent upon the fission-product pairs that are sampled for each fission event. This contrasts with binwise integration, wherein the 25-group energy structure is used for all fission-product CDFs. Thus, for example, for binary fission the energy CDFs depend on line-emission energies of all nuclides for the fission-product pair rather than a fixed bin structure. The **gg2** and **gg2_l** storage is thus done based on fission-product pairs for exact integration rather than individual fission products for binwise integration.

Exact integration feature is practical—from both storage and execution time perspectives—only if a few hundred emission lines are treated for each fission or residual-nuclide event. Our testing indicates that approximately 350 lines can be comfortably accommodated on PCs with 1 MByte of RAM.

As a second control option, a threshold factor, gsthresh, can be used to eliminate the "weakest" emission lines as the line data from cindergl.dat are processed during calculation initialization. This factor causes the elimination of all lines that are less than the factor gsthresh of the maximum line for an isotope; e.g., the value 5 would eliminate those lines that are <5% of the strength of the largest line on an isotope-by-isotope basis.

By eliminating weak lines for fissioning nuclides, our testing indicates that the number of emission lines reduced from thousands to fewer than 350 for fission events. However, for exact integration, **gg2** and **gg2_l** data can be stored for only the top few hundred fission-product pairs (on many modern computing platforms). Thus, **gg2** and **gg2_l** data for infrequently sampled fission-product pairs must be repeatedly calculated. Computational tests indicate that this strategy is highly viable because (1) execution time is reduced by 95% when the top fission-product-pair strategy is used to calculate (once) and reuse **gg2** and **gg2_l** data versus calculations wherein **gg2** and **gg2_l** are recalculated for each fission, and (2) line-by-line integration calculations can be executed using personal computers (not limited to larger platforms).

To illustrate, an MCNPX simulation made with a 25-group treatment of delayed gammas can require approximately 4 times more execution time than a simulation without delayed gammas. A simulation made using line data can require more than 10 times as much execution time than the no-delayed-particle calculation. Execution of a line-data simulation can be reduced by 50% using the gsthresh factor to eliminate the weakest 5% of the lines. As would be expected, execution times are model dependent, and can vary from minutes for 25-group models with approximately one million source histories on a 3-GHz, single-processor platform to days for high-fidelity line data models with ultra-fine energy binning executed with billions of source histories on clusters. To form CDFs storing information for all emission lines, perhaps a fifty-fold increase in RAM is necessary for commonly available computers (i.e., ~50 Gbyte). However, this is dependent on the number of line data and the desired fidelity.

4.5.2. Sampling recipe.

Delayed-gamma emission in MCNPX is performed according to the following recipe.

1. Sample the target and fission products or residual nuclides in **COLIDN**, **ACECOL**, **INTERACT**, **CID** (see Figs. 1a and 1b in the Appendix).
2. For each fission event, create CDF data using subroutines called by **CID** (see Figs. 1a and 1b in the Appendix). Store the CDF values in a look-up table.*
3. Sample the number of delayed gammas to be emitted in **DNG_MODEL**. This process is random, with the number of emitted gammas ranging from zero to

* In practice, memory limitations (for the "gg2_l" array) dictate that table look-up is limited to the most frequently sampled fission products. CDFs for lesser sampled fission products are recalculated as needed.

the integer value of the S given by Eq. (66), or nj = int($S + r$), where r* is a random number on **[0,1)**.† Then, for each delayed gamma to be emitted, the following steps are executed:

4. Randomly select the energy range of emission using Eq. (71) and searching until $r < \Xi^{ML}_{J,KS,\tilde{K}S}$ so that the emission energy index is $k = \tilde{K}S$.‡

5. Determine whether multigroup or line emission occurs according to whether $r < \Xi^{ML-M}_{J,\tilde{K}S} / (\Xi^{ML-M}_{J,\tilde{K}S} + \Xi^{ML-L}_{J,\tilde{K}S})$. If this condition is true, then multigroup emission occurs; otherwise, line emission results.

6. Determine emission energy. If multigroup emission occurs, sample the emission energy randomly in the energy interval so that $E_{emit} = E_{k-1} + r \times (E_k - E_{k-1})$, where the E_k are the energy bin limits for this CDF. For line emission via exact integration, the energy index from step 4 determines the emission line and **FIND_GAMMAL** is called to determine the identity of the emitting nuclide.

---

* A different random number r is used for each step in this recipe.

† This algorithm differs from that used for delayed-neutron sampling. For neutrons, the delayed and total number of neutrons created by a fission event is available from ACE library data ("dn" and "tn"). Thus, sampling can be done using a normalized CDF, i.e., for each i=1,nt where nt=tn+r, if r ≤ dn/tn, then a delayed neutron is sampled; otherwise, a prompt neutron is sampled. For gammas, the total number (prompt and delayed) of gammas created by a fission event is not available; thus, the sampling of delayed gammas is done without a normalized CDF involving the total number of gammas ("tg").

‡ Here and for the other sampling types, FORTRAN accommodation is made for the first and subsequent bins so that the proper bin limits are observed.

7. Determine emission time. For line emission involving a principal nuclide, sampling is done analytically using Eq.(63). Table lookup is done for either multigroup or non-principal-nuclide emission. If multigroup emission occurs, the sample according to Eq.(45), searching until $r < \Xi^{M}_{JS,K}$. Sampling for line emission involving a non-principal nuclide is done using Eq.(65) and finding $r < \Xi^{D-L}_{\tilde{i},JS,\tilde{n}}$. The delay time for table lookup is $t_d = t_{JS-1} + r \times (t_{JS} - t_{JS-1})$, where the t_j are the integration-bin boundaries. The emission time is then calculated as the time at which the fission event occurred plus the emission-delay time: $t_e = t + t_d$.

8. Determine emission direction. Randomly sample isotropic emission.

9. Once these steps are completed, these emission data are passed from the interface routine back to MCNPX, whereupon the actual process of the delayed-gamma transport is done. Once a delayed gamma is transported, control is returned to the interface routine. The emission-data-generation/transport process is repeated for each of the remaining delayed gammas that are emitted for this fission event.

10. After all delayed gammas are transported for a fission event, control is returned to MCNPX.

4.5.3. Analog versus nonanalog sampling.

At present, capability has been developed for analog sampling of delayed-gamma emission. Depending on the application and user need, the inability to perform nonanalog (variance reduction) sampling may result in the need for increased execution time in order to develop statistically reliable results.

4.6. Continuous-data integration scheme.

The continuous emission data are pointwise differential data given at 10-keV intervals. To obtain consistency with the discrete (integral) data, the continuous data are integrated over energy. The intra-bin behavior is presumed to vary linearly as a function of energy. The resulting integration scheme mirrors that discussed in Eq. (24).

4.7. Isotope/line identification scheme.

Capability has been implemented in MCNPX to associate the delayed gammas created via line emission with their emitting radionuclide. This identification is maintained throughout transport, including inelastic scatter. Consequently, each line-emission photon can be used to identify its source, provided that the photon is tallied.

5. SUMMARY AND CONCLUSIONS.

A major software development effort has been undertaken to provide MCNPX with new capability to automate the calculation of delayed-gamma emission spectra at discrete (line) energies for radioactive species created by neutron-induced fission and by activation (simple-multi-particle) reactions involving neutron absorption. This signature-

generation capability is fully time dependent, with the CINDER'90 isotopic transmutation code supplying isotopic concentrations for 3400 fission products. CINDER'90 is interfaced with MCNPX, allowing for seamless, streamlined execution without the need for the creation and manipulation of interface files. ENDF/B-VI evaluated line-emission data are supplied for 979 radionuclides; 25-group data are used for the balance of the 3400 nuclides.

The nuclide photon line-emission spectral data have been aggregated into a new file: cindergl.dat. These data include the gamma and x-ray data, consisting of 24000 discrete and 258000 continuous values, contained in the files maintained by LANL Group T-16 at http://t2.lanl.gov/data/decayd.html as extracted from the ENDF/B-VI evaluation. A new input routine has been created to input these data into MCNPX. Dynamically allocatable storage is used, which will simplify the incorporation and use of data for additional nuclides obtained from future evaluations.

The new delayed-gamma capability is a Monte Carlo technique. Thus, it involves the creation and sampling of CDFs for the fission products or residual nuclides, the number of delayed gammas produced for an event, and the energy, time, and direction of emission.

For lower energies, fission products are determined (sampled) for using fission-yield data for thermal, fission-spectrum (fast), and high-energy (>14 MeV) source-neutron energies.

Interactions for neutrons having energies in excess of 20 MeV are calculated using LAHET, which is also an integral piece of MCNPX, to produce a list of residual nuclides.

For each fission or activation event, time-dependent concentrations for decay-chain nuclides are calculated by CINDER'90 using the sampled fission products. Non-fission neutron-induced transmutation with mass conservation is not treated in the current upgrade. As such, this upgrade is most relevant for "fixed-source" modeling of pulsed or low-flux systems. Future effort is needed to treat time-dependent material behavior for prolonged-exposure or high-flux systems; i.e., linking the delayed-gamma and "burn" (Fensin et al., 2006) capabilities.

Delayed-gamma calculations may be executed using either multigroup or line/multigroup data.[†] Multigroup execution can suffice for lower-fidelity studies, whereas high-fidelity investigations require line/multigroup execution.

For line/multigroup execution, the lack of line data for all 3400 nuclides treated by CINDER'90 means that the new capability has to accommodate the line/multigroup data mixture. This accommodation has included the derivation and coding of hybrid CDFs which treat both line and multigroup components for all radionuclides produced by a fission or activation event (i.e., the fission products residuals and their radioactive decay products).

[†] Where "line-data" execution connotes the use of the 979-nuclide dataset, with the balance of the nuclides treated using multigroup data.

Multigroup execution is done using binwise integration for CDF evaluation. Line/multigroup execution is done using binwise or line-by-line integration for CDF evaluation. Binwise integration uses the 25-group cinder.dat gamma structure, and, for line/multigroup execution, lumps line data into the multigroup bins. The line-by-line (exact) scheme integrates the line data exactly for each fission event, while simultaneously breaking the multigroup data into a corresponding number of energy bins.

Care is taken to minimize or eliminate redundant CINDER'90 execution so as to speed the time-consuming calculations. Furthermore, when adequate storage is available (which is the case on modern personal computers having a minimum of several megabytes of RAM), CDF data are calculated for the first instance in which each fission-product is sampled. These data are stored for reuse in subsequent fission events producing previously sampled fission products. Issues involving CINDER'90 execution and CDF storage are handled internally by MCNPX, and are transparent to the user.

Importantly, the delayed-gamma feature has been developed in a manner that requires only a minor adjustment to the MCNPX user interface (i.e., the input deck). The user need only supply the customary (i.e., for models excluding delayed gammas) geometry, materials, inhomogeneous neutron and/or photon source(s) (i.e., the "sdef" card), and the cross-section-library specifications. A single entry on the "phys:p" card is all that is required to initiate delayed-gamma calculations. The standard time component structure of the tallies remains unchanged—times on the order of seconds can be entered on tally cards to obtain time-dependent delayed-gamma tallies.

MCNPX has the capability to identify each line in an emission spectra in terms of the nuclide(s) producing the line via tagging (McKinney, 2008). This line-nuclide association is maintained throughout transport. As is discussed in Part II, calculations have been executed to verify MCNPX line-identification functionality for the cindergl.dat data and to validate capability using measured data (Beddingfield and Cecil, 1998). However, identification correctness is also predicated on the validity of the ENDF/B-VI experimental data, the acquisition of which is a laborious process (Tipnis et al., 1998). Insofar as the cindergl.dat line data are valid, calculated MCNPX line identification is valid.

The user may specify neutron and/or photon sources (using the MCNPX "sdef" card) in the same manner as would be stipulated for simulations that exclude the delayed-gamma feature. Thus, if desired, simple to exotic source dependencies involving particle type, energy, space, direction, and/or time could be used to investigate the resulting fission-induced delayed signatures.

MCNPX is not a static code—its developers are constantly creating and upgrading features, and this is the case for the delayed-gamma capability. As is discussed in this paper, additional upgrades are either underway or planned that will further extend the MCNPX delayed-gamma capability. More notable upgrades include the creation and use of new photon-induced nuclear-reaction cross sections, new photofission yields (Durkee et al., 2009), activation reaction-based delayed-gamma emission using non-analog

capture, biased delayed-gamma emission, the introduction of a new input card that will contain execution controls, and the use of new delayed-neutron spectral-emission data (to bring the model calculation of delayed-neutron emission into accordance with the delayed-gamma emission technique).

Although the focus of this paper is on delayed-gamma production due to neutron-induced reactions, we should mention that the inclusion of the high-energy LAHET package in MCNPX enables the study of delayed-gamma emission arising from interaction of other types of high-energy particles with matter (Waters et al., 2008). LAHET produces residual nuclides for reactions involving the 34 types of source particles treated by MCNPX, which appreciably broadens the scope of problems for which delayed-gamma signature analysis can be conducted.

The new delayed-gamma simulation feature is powerful. It is capable of providing either low- or high-fidelity delayed-gamma signatures. In principle, execution is simple—requiring only a single entry on the MCNPX phys:p card in order to activate the feature. However, as is the case with all Monte Carlo tools, it is important that the user be mindful of the need to exercise care in its use. It is important to be aware that model setup and execution impacts the sampling of relevant quantities, including target nuclei, fission products or residual nuclides and their decay progeny, and delayed-gamma quantity, emission energy, time, and direction. Indeed, whereas many types of MCNPX simulations involve static isotopic quantities, the time-dependent behavior of the decay-chain atom densities for delayed-gamma simulations impacts simulation results in a time-

dependent manner. Tally makeup and results should thus be considered carefully. Tally adequacy is measured by the tally relative uncertainty and ten statistical checks. Because the delayed-gamma feature can require substantial execution time (hours to days on clusters), we recommend that initial simulations be done using simplified models with relatively coarse tally bins to assess results as a prerequisite for detailed modeling. We suggest that new simulation efforts initially exclude the use of models containing hyperfine tally bins in energy, time, or other parameters so as to avoid potentially poor or confusing results. Information gained from coarse-structure tallies can then be used to meaningfully implement fine-structure models.

Validation calculations are presented in Part II. The models are based on experiments performed by Fisher and Engle (1964) and Beddingfield and Cecil (1998) for neutron-induced fission. An activation result is also presented.

The reader should consult Part III for the presentation of a transport-theory formulation that we give as a means of conveying a succinct encapsulation of the relevant physics for the delayed-gamma feature. This presentation is a useful augmentation to the Monte Carlo formulation contained in Part I.

ACKNOWLEDGEMENTS

We gratefully acknowledge the support of DHS/DNDO.

6. REFERENCES.

Battat M.E., Dudziak D.J., and Johnston K. (November 1968), "Fission Product Heating in Fast Reactor Plutonium Fuel," J. of Nuclear Energy; v.22, pp. 703–704.

Beddingfield D.H. and Cecil F.E. (1998), "Identification of Fissile Materials From Fission Product Gamma-Ray Spectra," Nuclear Instruments and Methods in Physics Research A; v.417, pp.405–412.

Bevington P.R. and Robinson D.K. (1992), *Data Reduction and Error Analysis for the Physical Sciences*, McGraw-Hill, Inc. , pp. 81–90.

de Hoffmann F., Feld B.T., and Stein P.R. (November 15, 1948), "Delayed Neutrons From U^{235} After Short Irradiation," Physical Review, v.74, no. 10, pp. 1330–1337.

Durkee Joe W. Jr., McKinney Gregg W., Trellue Holly R., Waters Laurie S., and Wilson W. B. (2009), "Delayed-Gamma Simulation Using MCNPX," accepted for publication in Nuclear Technology.

England T.R., Wilson W.B., and Stamatelatos M.G. (December 1976), "Fission Product Data for Thermal Reactors. Part 1: A Data Set for EPRI-CINDER Using ENDF/B-IV," Los Alamos National Laboratory report LA-6745-MS.

England T.R. and Rider B.F. (October, 1994), "Evaluation and Compilation of Fission Product Yields," Los Alamos National Laboratory report LA-UR-94-3106.

Engle L.B. and Fisher P.C. (1962), "Energy and Time Dependence of Delayed Gammas From Fission," Los Alamos National Laboratory report LAMS-2642.

Erdtmann G. and Soyka W. (1979), *The Gamma Rays of the Radionuclides. Tables for Applied Gamma Ray Spectrometry*, Verlag Chemie, Weinheim, New York.

Estes G.P., Schrandt R.G., and Kriese J.T. (March 1988), "Automated MCNP Photon Source Generation for Arbitrary Configurations of Radioactive Materials and First-Principles Calculations of Photon Detector Responses," Los Alamos National Laboratory report LA-11153-MS.

Fensin M.L., Hendricks J.S., and Anghaie S., "Enhanced Monte-Carlo-Linked Depletion Capabilities in MCNPX," Los Alamos Report: LA-UR-06-0363, 2006 International Congress on Advances in Nuclear Power Plants Embedded Topical Meeting at the 2006 ANS Annual Meeting, ICAP '06, Reno, NV (June 4-8, 2006).

Fisher P.C. and Engle L.B. (1964), "Delayed Gammas From Fast-Neutron Fission of Th^{232}, U^{233}, U^{235}, U^{238}, and Pu^{239}," Physical Review B; v.134, no.4B, pp.B796-B816.

Frisch O.R. (September 27, 1945), "Controlled Production of an Explosive Nuclear Chain Reaction," Los Alamos National Laboratory report LA-397 (unclassified).

Goudsmit S.A. (1988), *ALSOS*, Tomash Publishers, American Institute of Physics, p. 13.

Griffin J.J. (1964), "Beta Decays and Delayed Gammas From Fission Fragments," Physical Review B; v.1, no.4B, p.34B817.

Guung T-C, Tsai W-F, Kuo W-S, and Chen, J-S (2002), "MCNP Simulation of TRR-II Cold Neutron Source Design," Physica B, v.311, pp.158–163.

Henderson D.L., Sawan M.E., Moses G.A. (1988), "Radiological Dose Calculations for the Diode Region of the Light Ion Fusion Target Development Facility," Fusion Technology, v.13, pp.594–615.

Henry A.F. (1975), *Nuclear-Reactor Analysis*, MIT Press, The Massachusetts Institute of Technology, p. 10.

Hollas C.L., Close D.A., and Moss C. E. (April 1987), "Analysis of Fissionable Material Using Delayed Gamma Rays From Photofission," Nuclear Instruments and Methods in Physics Research Section B: Beam Interactions With Materials and Atoms, v24-25, Supplement Part 1, pp. 503–505.

Jurney E.T., Bendt P.J., and England T.R. (January 1979), "Fission Product Gamma Spectra," Los Alamos National Laboratory report LA-7620-MS.

Katakura J. and England T.R., (1991), "Augmentation of ENDF/B Fission Product Gamma-Ray Spectra by Calculated Spectra," Los Alamos National Laboratory report LA-12125-MS.

Keepin G.R. (1965), *Physics of Nuclear Kinetics*, Addision-Wesley Publishing Company, Inc., London, pp. 145–159.

Klingensmith J.J. and Gauld I.C. (2005), "ORIGEN-S Gamma Decay Spectra Characterization and Benchmarking," Trans. Am. Nucl. Soc., 93, pp. 33–34.

Lamarsh J.R. (1972), *Introduction to Nuclear Reactor Theory*, Addision-Wesley Publishing Company, Inc., Reading, Massachusetts, pp. 92–94.

Liew S.L. and Ku L.P. (1991), "Monte Carlo Calculation of Delayed Gamma Does Rate in Complex Geometry Using the Concept of Effective Delayed Gamma Production Cross Section," Nuclear Science and Engineering, v.107, pp.114–130.

Ma R., Zhao X., Rarback H.M., Yasumura S., Dilmanian F.A., Moore R.I., Lo Monte A.F., Vodopia K.A., Liu H.B., Economos C.D., Nelson M.E., Aloia J.F., Vaswani A.N.,

Weber D A., Pierson R.N. Jr., and Joel D.D. (February, 1996), "Calibration of the Delayed-Gamma Neutron Activation Facility," Medical Physics, v.23, no.2, pp. 273–277.

Maienschein F.C., Peelle R.W., Zobel W., and Love T.A. (1958), "Gamma Rays Associated with Fission," Proceedings of 2nd International Conference Geneva, **15**, pp. 366–377.

Malenfant R. E. (August, 2005), "Experiments with the Dragon Machine," Los Alamos National Laboratory report LA-14241-H (unclassified).

McKinney G. W. (2008), "Tally Tagging Feature in MCNPX 2.7.A," LA-UR-08-04511, Proceedings of the ANS Winter Meeting, Reno, NV, November 9-13, 2008.

Moon P.B. (April 7, 1945), "Short-Period Delayed Gammas From Fission of 25," Los Alamos National Laboratory report LA-253 (unclassified).

Moore B.M. (October 1969), "Short-Lived Delayed Gamma-Ray Emission from Fast Fission of Plutonium," Los Alamos National Laboratory report LA-4257.

Morgan K.Z. and Turner J.E. (1973), *Principles of Radiation Protection*, Robert E. Krieger Publishing Company, Huntington, New York, pp. 31–49.

Norman E.B., Prussin S.G., Larimer R., Shugart H., Browne E., Smith A.R., McDonald R.J., Nitsche H., Gupta P., Frank M.I., and Gosnell T.B. (2004), "Signatures of Fissile Materials: High-Energy γ Rays Following Fission," Nuclear Instruments and Methods in Physics Research A; v.521, pp.608–610.

Pelowitz D.B., ed. (April 2008), "MCNPX User's Manual Version 2.6.0," Los Alamos National Laboratory report LA-CP-07-1473.

Pruet J., Hall J., Descalle M.A., and Prussin S. (2004), "Monte Carlo Models for the Production of β -Delayed Gamma-Rays Following Fission of Special Nuclear Materials," Nuclear Instruments and Methods in Physics Research B; v.222, pp.403–410.

Roberts R.B., Meyer R.C., and Wang P. (1939), "Further Observations on the Splitting of Uranium and Thorium," Physical Review; v.55, pp.510–511.

Siciliano E.R., Ely J.H., Kouzes R.T., Milbrath B.D., Schweppe J.E., and Stromswold D.C. (2005), "Comparison of PVT and NaI(Tl) Scintillators for Vehicle Portal Monitor Applications," Nuclear Instruments and Methods in Physics Research A; v.550, pp.647–674.

Slaughter D.R., Accatino M.R., Bernstein A., Dougan A.D., Hall J.M., Loshak A., Manatt D.R., Pohl B.A., Walling R.S., Weirup D.L., and Prussin S.G. (August, 2005), "The 'Nuclear Car Wash': A Scanner to Detect Illicit Special Nuclear Material in Cargo Containers," IEEE Sensors Journal; v.5, no. 4, pp.560–564.

Spletzer B.L. (1992), "The Delayed Gamma Environment Produced by Exoatmospheric Nuclear Weapons Detonation (U)," Sandia Report SAND91-0285.

Szasz F.M. (1984), *The Day the Sun Rose Twice*, University of New Mexico Press, Albuquerque, pp. 115–144.

Tipnis S.V., Campbell J.M., Couchell G.P., Li S., Nguyen H.V., Pullen D.J., Schier W.A., Seabury E.H., and England T.R. (1998), "Yields of Short-Lived Fission Products Produced Following $^{235}U(n_{th},f)$," Physical Review C; v.58, no.2, pp.905–915.

Trellue H.R., McKinney G.W., and Durkee J. (2005), "Burnup Capability Added to MCNPX," American Nuclear Society 2005 Annual Meeting.

Way K. and Wigner E.P. (1948), "The Rate of Decay of Fission Products," Physical Review; v.73, no.11, pp.1318-1330.

Waters L.S., ed. (November 19, 1999), "MCNPX User's Manual Version 2.1.5," Los Alamos National Laboratory report TPO-E83-G-UG-X-00001.

Waters L.S., Durkee J.W., Elson J.S., Esch E.I., Fensin M.L., Hendricks J.S., Holloway S.T., James M.R., Jason A., Johns R.C., Johnson M.W., Kawano T., McKinney G.W., Moller P. and Pelowitz D.B. (2008), "MCNPX Improvements for Threat Reduction Applications," LA-UR-08-05737 and Proceedings of the 20th International Conference on the Application of Accelerators in Research and Industry, CAARI2008 American Institute of Physics Conference Proceedings Series (accepted).

Weidenspointner G., Harris M. J., Sturner S., and Teegarden B.J. (January, 2005), "MGGPOD: A Monte Carlo Suite for Modeling Instrumental Line and Continuum Backgrounds in Gamma-Ray Astronomy," The Astrophysical Journal Supplement Series, v.156, pp.69–91.

Wilson W.B., England T.R., George D.C., Muir D.W., and Young P.G. (1995), "Recent Development of the CINDER'90 Transmutation Code and Data Library for Actinide Transmutation Studies," Los Alamos National Laboratory report LA-UR-2181.

Wilson W.B., England T.R., Arthur E.D., Beard C.A., Bowman C.D., Engel L.N., Gavron A., George, D.C., Daemen L.L., Hughes, III H.G., Kinnison W.W., LaBauve R.J., Lee D.M., Lichtenstein H., Lisowski P.W., Muir, D.W., Palounek A.P., Perry R.T., Pitcher E.J., Prael R.E., Russell G.J., Sanders G., Waters L.S., Young, P.G, and Ziock H.J. (January 11–15, 1993), "Accelerator Transmutation Studies at Los Alamos with LAHET, MCNP, and CINDER'90," Proceedings of the Workshop on Simulating Accelerator Radiation Environments.

APPENDIX

A block diagram is given in Fig.1a to help illustrate the basic MCNPX code flow for neutron-induced fission production of delayed gammas and neutrons. Blocks shown in blue are existing higher-level routines. Yellow and brown blocks are low- and high-energy routines for calculating neutron interactions with a nucleus. Red blocks relate to CINDER'90, including data and CDF calculation. Green blocks represent the delayed-gamma emission routines. The comments within each block are limited to the briefest possible functionality concepts relevant to delayed-gamma (and neutron) emission.

Figure 1a shows that the calculation begins in **MAIN** with problem input. **IMCN** is then called for multitasking and multiprocessing setup, the input of delayed-particle data in **LIBPREP** (multigroup) and **LIBGAMMA_LINES**, and particle-transport initialization and coordination of output; **TRNSPT** is called for particle transport; and **HSTORY** is called for cross-section generation and coordination of particle tracking. Subroutine **COLIDN** treats source neutron transport, calling **ACECOL** for sub-20-MeV interactions, and calling **INTRCT** and **INTERACT** for high-energy interactions. **DNG_MODEL** is called by **COLIDN** for each fission event; **DNG_MODEL** does the delayed-particle emission (particle type and number, energy, time, and direction). **CINDER_INTERFACE_DELAYEDNG (CID)** serves as the MCNPX/CINDER'90 interfacing routine. CDF information is assembled in **CID** using data from CINDER'90 for use in **DNG_MODEL**.

Figure 1b shows code flow inside of **CID**. **CID** calls **CID_SAMPF1** for each fission product or residual nuclide. **CID_SAMPF1** calls CINDER'90 and uses the time-dependent atom densities to calculate the multigroup and/or line CDF components (gg2, gg2_l, Eqs.(34) and (58), and dgval, dgval_l, Eqs.(31) and (55)), as well as to store the emission energies (espkgl_cdf) and the nuclide-association data for this CDF. For exact integration involving a pair of fission products, **GETFPPAIR_ID** is called to obtain the matrix-storage identity information that is used to store CDF information according to fission-product pairs. Memory permitting (<350 emission energies for a fission-product chain), these data are stored for reuse (_fpc arrays) so that sampling of the same fission product for subsequent fissions will avoid calls to **CID_SAMPF1** and CINDER'90. If a fission product has a lengthy chain, these data are recalculated by **CID_SAMPF1** for subsequent fissions. On return from **CID_SAMPF1**, the line data for the fission products or residual nuclides are sorted using **SORT_THREE_1DARRAYS** and then loaded (_fpc arrays) in **LOAD_LINES_THISFPC**.

Once all fission-event CDF energies are loaded, **SORT_THREE_1DARRAYS** is called to sort the CDF lines in order of increasing energy and to rearrange two emission-identification arrays concurrently to enable the tagging of each line-emission delayed gamma. The line data for both fission products or all residual nuclides are then assembled in **LOAD_LINES_THISCDF**. Next, **CID_SAMPF2** calculates the total number of delayed gammas emitted as a function of time for multigroup and line data (totg, totg_l) as well as the delayed-neutron data (totn). Finally, **CID_SAMPF3** makes the multigroup and line components of the CDFs (cdfge,cdfge_l, Eqs.(43), (61), and (71)).

The CDF data are returned to **DNG_MODEL** for use in delayed-gamma emission. The number of delayed gammas is sampled, followed by energy-emission sampling. The energy sampling accounts for multigroup and line-emission components. If line emission occurs, randomly sampled emission energy is sent with the CDF emission-energy array to **FIND_GAMMAL,** where the appropriate emission line energy is obtained. This emission process is repeated for each delayed gamma emitted for a fission or simple-multi-particle event.

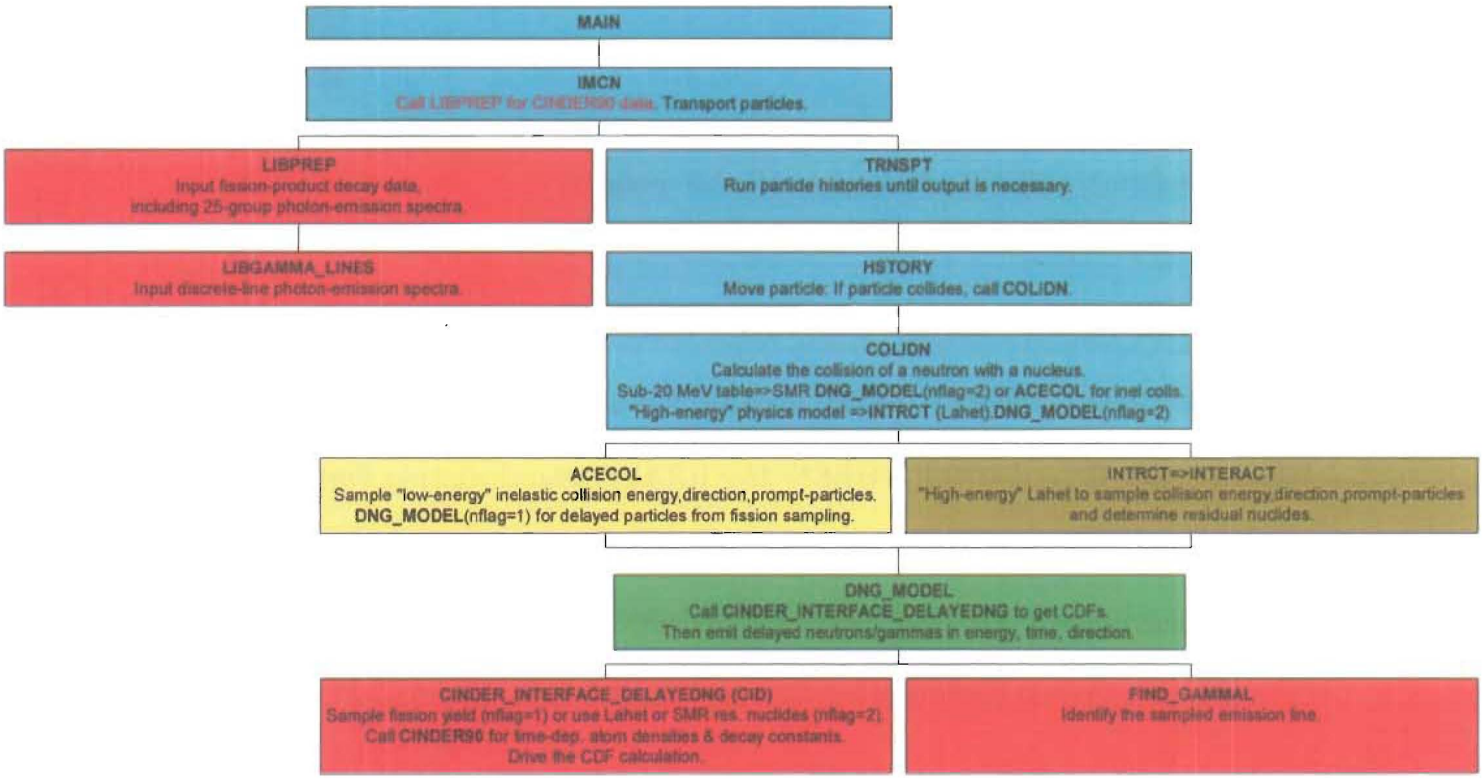

Figure 1a. General MCNPX code flow for neutron-induced delayed neutron/gamma creation.

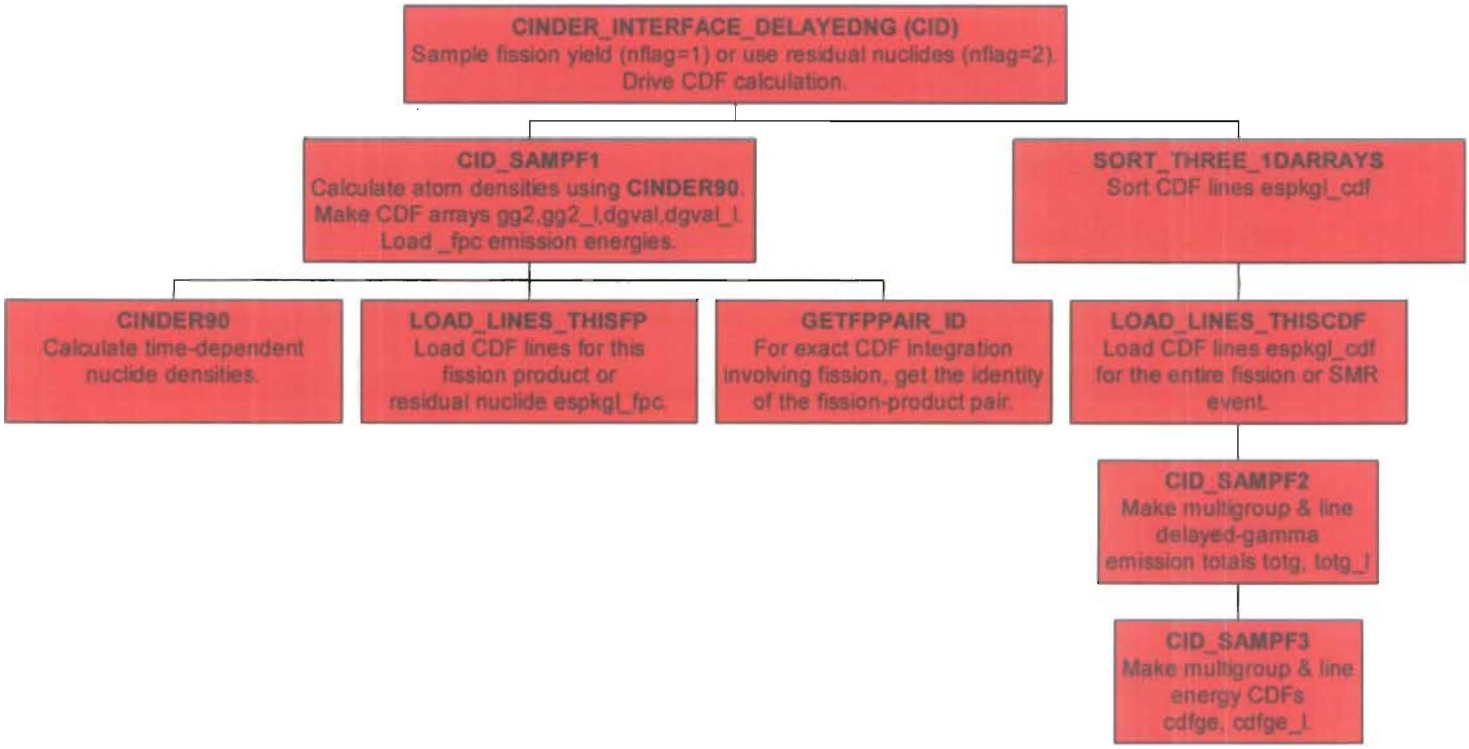

Figure 1b. Primary MCNPX delayed-gamma subroutines.

Routines **LIBGAMMA_LINES, CID, CID_SAMPF1, CID_SAMPF2, CID_SAMPF3, FIND_GAMMAL, LOAD_LINES_THISFP, LOAD_LINES_THISCDF, GETFPPAIR_ID,** and **SORT_THREE_1DARRAYS** are included in a Fortran 90 module named **CINDER.** Subroutine **DNG_MODEL** is external to the module to interface conveniently with other portions of MCNPX. Including CINDER'90 and comments, the upgrade consists of approximately 20,000 lines of Fortran 90.

LIST OF TABLE CAPTIONS

Table 1. Line-data composition for 979-radionuclide delayed-gamma dataset

LIST OF FIGURE CAPTIONS

Figure 1a. MCNPX general code flow for neutron-induced delayed neutron/gamma creation.

Figure 1b. Primary MCNPX delayed-gamma subroutines.